Summary

We propose to build the Very Energetic Radiation Imaging Telescope Array System (VERITAS), an array of seven 10 m aperture optical reflectors for γ-ray astronomy in the 50 GeV to 50 TeV energy range. These atmospheric Cherenkov telescopes will use the imaging concept developed by the Whipple Observatory Gamma-Ray Collaboration and used to detect the first galactic and extragalactic sources of TeV γ-rays but will achieve an order of magnitude better sensitivity and a significant reduction in energy threshold. The new telescopes will improve upon the design of the existing Whipple Observatory 10 m telescope. Each telescope will have a tessellated 10 m mirror and long focal length (12 m) with the optical design optimized for good angular resolution, a large field of view, and minimum wavefront distortion. Each telescope camera will have 499 pixels covering a 3.5° field of view with 0.15° resolution. The detectors and camera electronics will use the most advanced technology currently available. The array will have an effective collection area in excess of 100,000 m^2 at energies above 1 TeV. VERITAS will be located in southern Arizona where it will take advantage of the existing infrastructure of the Whipple Observatory. With stereoscopic imaging, the array will achieve unprecedented angular resolution, energy resolution and background rejection over three decades of energy. The primary scientific objectives of VERITAS will be the study of active galactic nuclei, supernova remnants, pulsars, and γ-ray bursts and the search for new astrophysical sources. The minimum detectable flux sensitivity will be 0.5% of the Crab Nebula at 200 GeV, a factor of 20 improvement over the most sensitive telescopes currently operating in this energy range. The angular resolution ($<0.05°$) will be sufficient to identify a number of the unidentified sources detected by EGRET on the Compton Gamma Ray Observatory. VERITAS provides a unique combination of large collection area, low background, and good energy resolution. It will effectively complement GLAST, the next major high energy γ-ray telescope in space; together they may solve the problem of the origin of the cosmic radiation as well as probing fundamental questions in physics and cosmology. The capital cost of VERITAS is $21M and it can be built in five years.

Contents

1 Introduction

1.1 VHE Gamma-ray Astronomy

The Very Energetic Radiation Imaging Telescope Array System (VERITAS), the new telescope array proposed here, represents a dramatic step forward in the study of extreme astrophysical processes in the universe. It will substantially increase the catalog of very high energy (VHE, E$\gtrsim$100 GeV) γ-ray sources and greatly improve measurements of established sources. The field of ground-based γ-ray astronomy has been revolutionized by the power of the atmospheric Cherenkov imaging technique for the discovery and study of individual sources. This technique was largely developed by the Whipple Observatory Gamma-Ray Collaboration. Although less than 1% of the sky has been surveyed by the imaging technique at 300 GeV, thirteen sources have now been reported (eight with high significance) by ground-based groups using the imaging technique: three pulsar-powered nebulae, six BL Lacertae-type active galactic nuclei (AGN), three shell-type supernova remnants, and one X-ray binary system (Weekes 1999). These measurements have advanced our understanding of the origin of cosmic rays, the nature of AGN jets, the density of the background infrared (IR) radiation, and the magnetic fields in the shells and nebulae of supernova remnants.

Gamma rays are unique probes of the Universe. Unlike radiation at longer wavelengths, γ-rays are not attenuated significantly within the Galaxy. As such, they provide an unobstructed view through the plane of the Galaxy except for regions which contain high densities of low energy photons (or virtual photons in regions of high magnetic fields) where VHE γ-rays are attenuated via photon-photon pair production. Thus, the regions where the high energy γ-rays are emitted must have relatively low photon densities (e.g., in active galactic nuclei) or low magnetic fields (e.g., near a pulsar light-cylinder). For γ-rays from extragalactic sources, pair production with low energy photons can be used to probe intergalactic radiation fields. Finally, VHE γ-rays are typically at or near the end of the electromagnetic emission spectra of the objects which produce them, so the VHE γ-ray emission characteristics are often the most sensitive to the parameters used in the emission models and they probe the most energetic range of the underlying physical processes.

1.2 Next Generation Telescopes

The exciting advances made by the present generation of imaging telescopes (second generation systems) justify the construction of arrays of imaging telescopes (third generation systems). Such systems should have the following properties:

- *Larger effective area*: $\gtrsim$0.1 km^2 to provide sensitive measurements of short variability time-scales.
- *Better flux sensitivity*: detection of sources which emit γ-rays at levels of 0.5% of the Crab Nebula at energies of 200 GeV in 50 hours of observation.
- *Reduced energy threshold*: an effective energy threshold of $\lesssim$100 GeV with significant sensitivity at 50 GeV.
- *Improved energy resolution*: an RMS spectral resolution of $\Delta E/E \lesssim 0.15$ over a broad energy range.
- *Increased Angular Resolution*: $\lesssim$0.05° for individual photons; source location capability will be better than 0.005°.
- *Increased Field of View:* larger than the 3° diameter used in many current atmospheric Cherenkov imaging telescopes.

As we will show in this proposal, all of these objectives can be achieved simultaneously by building an array of imaging telescopes similar to the existing Whipple 10 m imaging telescope (Figure 1). VERITAS was first proposed in 1996 to the Smithsonian Institution. The concept has been presented at a number of conferences and a detailed description of it was given in the proposal presented to SAGENAP, the DOE/NSF Advisory group, in March, 1999.

1.3 VERITAS Philosophy

The philosophy underlying VERITAS comes from 30 years of development of atmospheric Cherenkov telescopes at the Whipple Observatory; the objective is to build a VHE γ-ray observatory which will have a useful lifetime well into the next century. The field of ground-based γ-ray astronomy has grown rapidly in the last decade due to the exciting discoveries by EGRET and Cherenkov telescopes. This growth is reflected in the composition of the VERITAS project. A number of new groups have joined the original Whipple Collaboration to formulate this proposal. These groups bring important technical expertise that will allow the expanded collaboration to carry out a project of this scale.

The VERITAS proposal is to build an array of seven telescopes of 10 m aperture; each telescope will be closely based on the proven design of the Whipple 10 m optical reflector. The power of arrays of imaging telescopes has been demonstrated and recently discussed in the literature (Krennrich et al. 1998; Konopelko et al. 1999).

The detailed design of VERITAS is based on the following considerations:

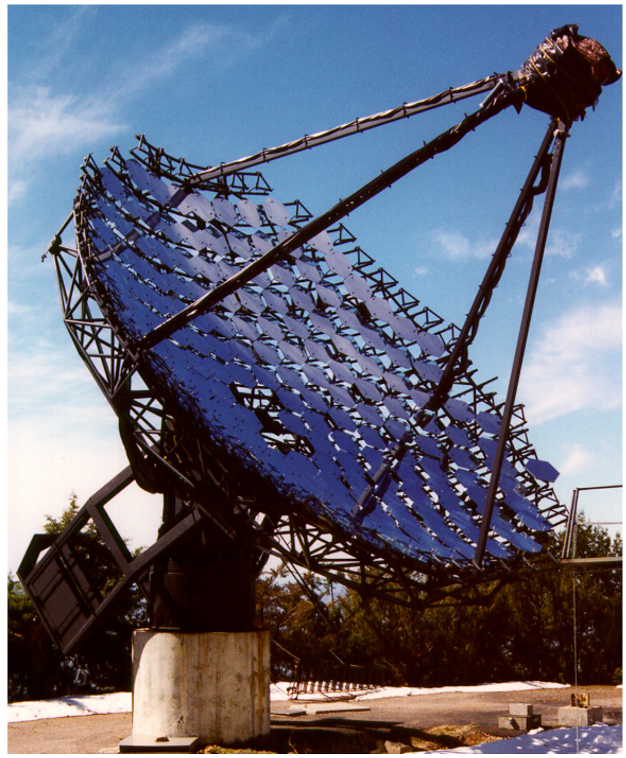

Figure 1: The Whipple Observatory 10 m reflector: the prototype for telescopes in VERITAS.

- *Proven technique:* The method of detection will be the atmospheric Cherenkov imaging technique which is now under considerable development at a number of centers.
- *Proven Technology:* The experience gained in the construction and operation of the 10 m reflector (built in 1968) and the camera (built 1987-99) will be adhered to wherever possible. However, we will incorporate significant innovations introduced by ourselves and our colleagues at other observatories if they have proven to be effective.
- *Modular Construction:* We will build one prototype telescope as quickly as possible and demonstrate that it meets its design criteria at the new site. The existing 10 m telescope will be operated throughout the construction phase and will serve as a test-bed for innovative technologies; it may ultimately become an eighth, non-standard element of the array. By building the additional telescopes over a five year period, we hope to be operational at all times.
- *Versatility:* With an array many experimental configurations are possible. The maximum sensitivity is achieved when all telescopes are operated in parallel, but there will be instances when different operating modes will be desirable. These vary from operation as discrete telescopes which monitor several sources, to operation of sub-arrays which obtain accurate measurements of stronger sources. It will also be possible to test experimental configurations in coincidence with normal telescope operation.
- *Location:* The array should be located where it has high operating efficiency, the construction costs are modest and there is existing infrastructure. Arizona offers some of the best observing conditions in the world and has the advantage of easy accessibility to most of the participating institutions. The Smithsonian Institution is a major sponsor of the project and there are suitable dark sites close to the Whipple Observatory which will provide the necessary infrastructure.
- *Cost:* The capital cost of the proposed facility will be larger than that of any previously built ground-based γ-ray observatory, but economical in terms of scientific return. The cost of VERITAS (Section 7) will be less than 10% of the GLAST mission, now estimated to cost at least $300 million.

2 Scientific Motivation

2.1 Active Galactic Nuclei

Active galactic nuclei (AGN) are galaxies with an unresolved central nucleus that outshines the rest of the galaxy and for which the emission is often dominated by nonthermal processes. Their emission is widely believed to be powered by accretion onto a supermassive black hole. The only AGN detected at γ-ray energies

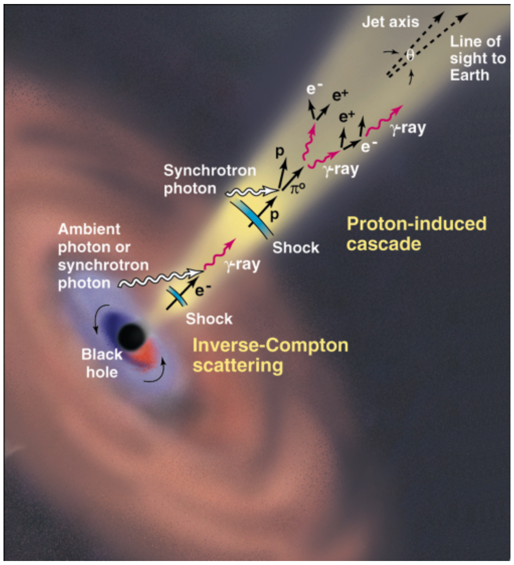

Figure 2: Artist's conception of the nucleus of an active galaxy. Two possible scenarios for the production of γ-rays in a relativistic jet are indicated (from Buckley 1998).

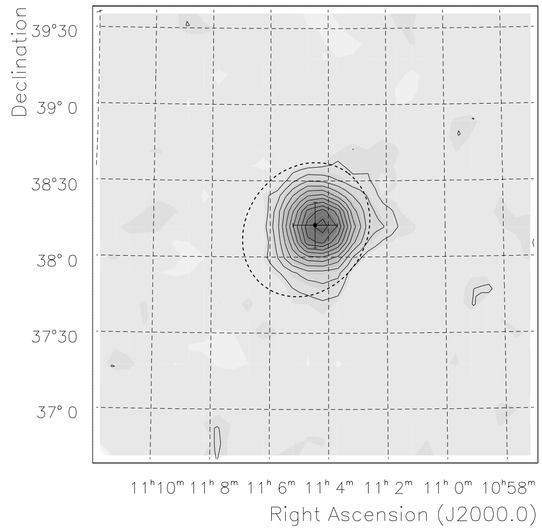

Figure 3: The VHE γ-ray emission from Mrk 421 (from Buckley et al. 1996). The solid contours are 2σ excess levels (the second contour is the 99.7% confidence region for the source location). The dashed ellipse is the 95% confidence interval determined by EGRET. The cross indicates the position of Mrk 421.

are blazars: radio-loud, flat spectrum sources characterized by highly variable and primarily non-thermal emission at most wavelengths. Flat spectrum radio quasars and BL Lacertae objects (BL Lacs) are members of the blazar class of AGN. The rapid variability and radio properties of these objects imply that they have relativistic jets whose axes make small angles with respect to the observer's line of sight. The γ-ray emission from these objects is also most naturally explained as beamed radiation from the jets which is Doppler boosted in energy and luminosity. Currently, no model for the production of γ-rays in the AGN is generally accepted. The two most popular classes are those in which high energy electrons (known to be present in the jets from radio, optical, and X-ray observations) produce the γ-rays by inverse Compton scattering of low energy photons and those in which very high energy protons produce the γ-rays by initiating cascades within the jets. These two processes are illustrated schematically in Figure 2.

Whipple observations of Markarian 421 (Mrk 421; Figure 3) and Mrk 501 have revealed extremely variable VHE emission (Figure 4; Quinn et al. 1999; Gaidos et al. 1996). Variability on a 15 minute time-scale observed in Mrk 421 (Gaidos et al. 1996) implies a compact emission region of dimension $R \lesssim 10^{-4}$ parsec (pc) which is only an order of magnitude larger than the radius of the event horizon of a 10^8 solar mass black hole. The emission region might exist at a somewhat greater distance from the central object (e.g., at a shock front propagating out along the jet), but this emission still originates well inside the ~1 pc region directly imaged by current radio telescopes. Correlations observed between X-rays and VHE γ-rays (e.g., Figure 4; Macomb et al. 1995; Buckley et al. 1996; Catanese et al. 1997) are most easily explained as emission at both wavelengths being produced by the same population of electrons. However, models which produce γ-rays primarily through proton interactions (Mannheim 1993) can also explain the observations. The combined low energy and VHE data provide quantitative constraints on jet parameters such as the magnetic field strength and Doppler factor. Whipple and EGRET observations have also led to reformulations of blazar unification models based on intrinsic source luminosity rather than solely on the effects of orientation differences (Ghisellini et al. 1998; Georganopoulos & Marscher 1998).

Despite these gains, we have much to learn about these enigmatic objects. VERITAS can help answer many of the unknowns concerning blazars, particularly when combined with lower energy observations by GLAST, X-ray and optical telescopes. We will approach the study of AGN from two perspectives: detailed studies where we conduct long observations of individual objects to reveal the physics operating in the AGN, and broad studies where we detect more VHE sources to illuminate patterns among various objects.

Detailed studies: The large effective area of VERITAS enables accurate measurements of extremely short variations in the γ-ray flux as illustrated in Figure 5. The left part of the figure shows Whipple observations of the fastest flare ever recorded at γ-ray energies. While the flare is clearly detected, the structure of the flare is not resolved. The dashed curve in the figure is a hypothetical flux variation which matches the Whipple data. The right part of the figure shows a simulation of what VERITAS would detect above 200 GeV. All features of the flare are clearly resolved. Space-based telescopes do not have the effective area to map out such low amplitude flares (GLAST would detect ~3 photons above 1 GeV from a flare of this duration and power). The broad energy coverage of VERITAS will also allow energy-dependent time delays to be resolved. These short time-scale measurements provide information about the acceleration, energy loss, and flaring processes in the jet, the location of the γ-ray emission, the jet characteristics, and even ambient photon levels and accretion rates for the central AGN.

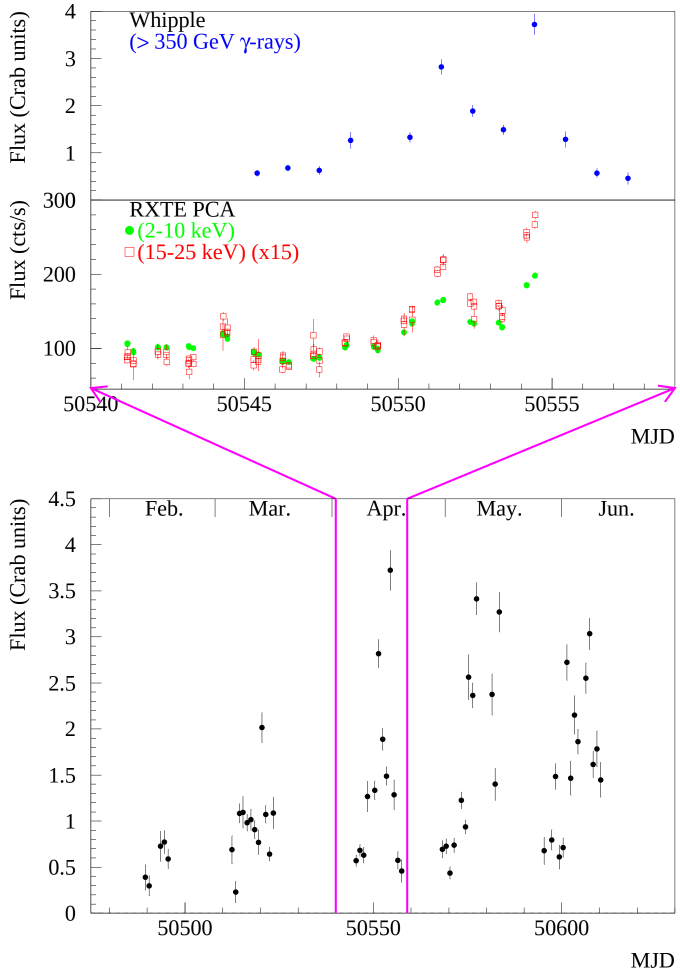

Figure 4: *Upper panel*: Observations of Mrk 501 in VHE γ-rays (top) and X-rays (bottom) taken during 1997 April 2-20 (April 2 corresponds to MJD 50540). Figure adapted from Catanese (1999). *Lower panel*: Average daily γ-ray rates observed with Whipple for Mrk 501 in 1997. Figure from Quinn et al. (1998).

Because of the extreme variability of blazars at all wavelengths, the best way to understand the physical processes at work in them is to conduct detailed observations spanning a wide energy range. A crucial requirement of these studies is consistent, dense temporal coverage of the object being studied. VERITAS can be divided into two dedicated sub-arrays of 3-4 telescopes, with one sub-array observing a single object for as long as it is above the 30° observation "horizon" for as many nights as the multi-wavelength campaign lasts. Thus, VERITAS can provide more complete measurements of flaring activity and greatly increase the chance of seeing a wide range of activity in the objects studied. The sensitivity of VERITAS to short-time scale variations will be an excellent match to X-ray and optical telescopes, permitting much improved measurements of energy-dependent variability. The wide energy coverage and good energy resolution of VERITAS will improve measurements of the blazar's spectral energy distribution and variability (particularly when combined with GLAST). Both are rather poorly constrained at this time but are critical to understanding the emission and flaring mechanisms. Finally, the flux sensitivity of VERITAS (and its ability to observe these objects consistently over long periods of time) will permit measurements of the baseline emission level in blazars, of which essentially nothing is presently known in the γ-ray regime.

Broad studies: The improved flux sensitivity of VERITAS will permit the detection of weaker sources of VHE emission. Its lower energy threshold will permit the viewing of objects further from Earth (the optical depth for pair production decreases rapidly with decreasing energy) and those objects which have spectral cut-offs below the sensitive range of existing Cherenkov telescopes. Based on the multi-wavelength spectra of Mrk 421 and Mrk 501, we expect that VERITAS will detect 30 or more X-ray selected BL Lacs. This should permit class-wide studies of this type of blazar that actually appears to be most efficient at emitting

VHE photons. An exciting prospect is that VERITAS will detect "Extreme BL Lacs," a hypothetical class of object whose power output actually peaks in the TeV range (Ghisellini 1999). These objects would be difficult to identify through traditional means (radio, optical, X-ray surveys) because of their low luminosity in those wavebands, but a detection at VERITAS energies would firmly identify them as blazars.

EGRET sources associated with AGN now number at least 66 (Hartman et al. 1999) and span a range of redshifts from $z = 0.03 - 2.28$, while only six AGN have been detected above 300 GeV. The most likely causes of this disparity are intrinsic cut-offs in the source spectra and, for the more distant sources, attenuation of the TeV γ-rays by pair-production with background IR radiation. The low energy threshold and good sensitivity of VERITAS will overcome these hurdles and lead to the detection of approximately 15 of the EGRET AGN, more if GLAST or all-sky X-ray monitors indicate when these objects are in high emission states. By measuring the ends of the spectra for several EGRET sources, VERITAS can help determine what particles produce the γ-ray emission in blazars (on average, electrons should show cut-offs which correlate with lower energy spectra, protons would not show a simple correlation). In addition, recent models to unify the different classes of blazar (Ghisellini et al. 1998; Georganopoulos & Marscher 1998) can be significantly refined or eliminated once the shapes and locations of the blazar spectra are measured. VERITAS is in a unique position to make these measurements, providing better photon statistics than space-based telescopes at these energies and superior energy resolution and sensitivity relative to other ground-based telescopes.

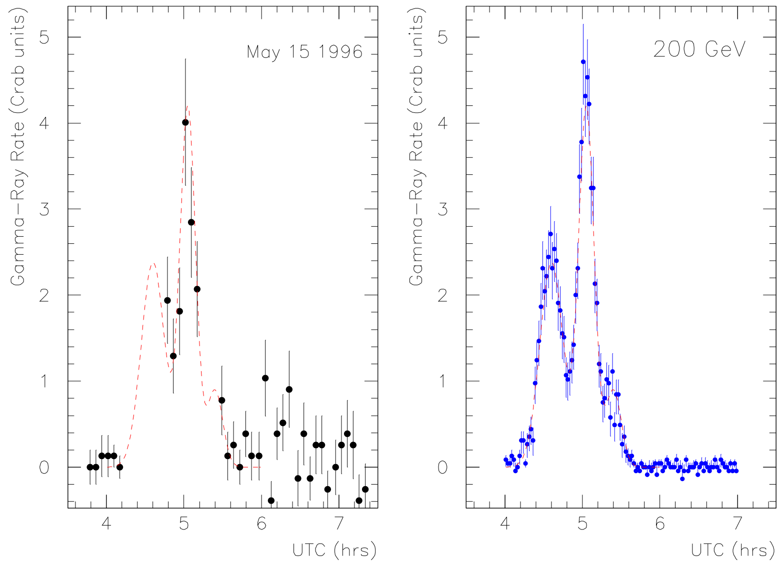

Figure 5: *Left:* Whipple observations of a rapid flare from Mrk 421 on 1996 May 15 (Gaidos et al. 1996). The superimposed dashed curve is a possible intrinsic flux variation which is consistent with the VHE data. *Right:* Simulated response of VERITAS to such a flare above 200 GeV.

2.2 Shell-type supernova remnants and cosmic rays

Supernova remnants: SNRs are widely believed to be the sources of hadronic cosmic rays up to energies of approximately $Z \times 10^{14}$ eV, where Z is the nuclear charge of the particle. This belief is supported by the fact that supernovae are the only galactic objects which appear to be capable of supplying the energy required for cosmic-ray generation. Also, the fairly well understood process of first-order Fermi acceleration (e.g., Blandford & Ostriker 1978) predicts the generation of high energy cosmic rays in supernova shock fronts and leads to power law energy spectra matching those inferred from cosmic-ray observations (e.g., Swordy et al. 1990). The existence of energetic *electrons* is well-known from observations of synchrotron emission at radio and X-ray energies (e.g., Koyama et al. 1995). Recently, the detection of TeV γ-rays from the shell-type SNRs SN 1006, RXJ 1713.7-3946 and Cassiopeia A has been reported (Weekes 1999). Unlike at X-ray and radio wavelengths, the TeV emission mechanism in these objects is unknown (e.g., Aharonian & Atoyan 1999; Baring et al. 1999). In addition to hadronic cosmic rays, electrons in SNRs may produce γ-rays via non-thermal bremsstrahlung and inverse Compton scattering of low energy photons. When combined with X-ray and radio observations, the VHE γ-ray observations provide a means of resolving these various contributions and providing information about SNR shell environments such as the maximum particle energy and magnetic field. Both are important but unknown parameters in shock acceleration theories.

Thus, a clear indication for the acceleration of hadronic particles in SNRs is still missing. The evidence for such processes would be γ-ray spectra characteristic of π^0 decay subsequent to nuclear interactions in the SNR. The γ-ray energies should range from $\sim$10 MeV up to ten's of TeV ($\sim$1/10 of the maximum proton energy), and the energy spectrum should follow the energy spectrum of cosmic rays in the source (thought to be a power law spectrum with index ~-2.1). While EGRET has detected signals from several regions of the sky consistent with the positions of shell-type SNRs (Sturner & Dermer 1995; Esposito et al. 1996; Lamb & Macomb 1997; Jaffe et al. 1997), its limited angular resolution makes definitive identification difficult. In addition, background from the diffuse Galactic γ-ray emission complicates spectral measurements.

The Whipple Collaboration has searched for γ-rays from several shell-type SNRs, but no emission has been detected (Buckley et al. 1998). Figure 6 shows the EGRET measurements and Whipple upper limits for the SNR IC 443. These results already eliminate much of the allowed parameter space for γ-ray emission from these objects (from hadrons and electrons), and begin to raise some questions about the validity of current models for the objects studied or for the propagation of cosmic rays.

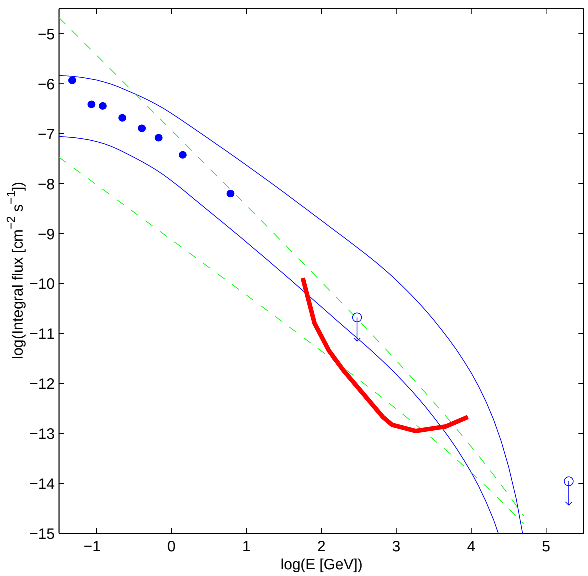

Figure 6: Predicted γ-ray spectra in the shell-type SNR IC 443. The region between the solid lines depicts the spectra from hadronic interactions for a range of model parameters (adapted from Buckley et al. 1998). The region between the dashed lines is the predicted inverse-Compton spectra for B between 20 μG and 50 μG and the range of flux normalizations and electron spectra allowed by the X-ray observations. EGRET data points (filled circles) and the current upper limits (open circles) from Whipple and the Cygnus air shower array are shown. The sensitivity of VERITAS for a 50 hour observation of this object is indicated by the thick curve.

As shown in Figure 6, there are predictions for strong γ-ray emission from shell-type SNRs by hadron *and* electron interactions. Model fits to EGRET and Whipple data (e.g., Gaisser et al. 1998) indicate that if the emission detected by EGRET is from the SNR, the combination of EGRET spectra and Whipple upper limits imply contributions from inverse Compton and bremsstrahlung scattering of electrons as well as hadronic interactions. They also require a relatively steep spectrum compared with the $E^{-2.1}$ expected from direct measurements. Resolving these various components will require accurate measurements over a large range of energies. VERITAS and GLAST will provide excellent sensitivity and energy resolution over more than six orders of magnitude in energy for the study of these objects. In addition, the excellent angular resolution of VERITAS will allow detailed mapping of the emission regions in the SNRs. For a typical SNR luminosity and angular extent, VERITAS should be able to detect objects within 4 kpc of Earth according to one popular model of γ-ray production by hadronic interactions (Drury et al. 1994). Approximately, twenty shell-type SNRs with known distances lie within this distance range, permitting VERITAS to investigate which characteristics of SNR are necessary for them to be sites of particle acceleration.

Diffuse galactic γ-ray emission: Cosmic rays interacting with the interstellar medium (ISM) give rise to the emission of γ-rays over a wide range of energies. The main processes are bremsstrahlung and inverse Compton scattering of electrons, and π^0 decay subsequent to hadronic interactions of protons and nuclei. Thus, observations of the diffuse galactic γ-ray emission, together with measurements of the arriving cosmic-ray flux, provide a unique probe of the distribution of both the ISM and the cosmic rays within the Galaxy. Observations with EGRET below 1 GeV agree well with models of the distribution of interstellar matter (Hunter et al. 1997). At higher energies, the observed γ-ray intensity exceeds the model predictions by $\gtrsim$50%. This excess could be due to unresolved point sources below the EGRET detection threshold, or it may reflect limitations in our understanding of cosmic rays, such as a local cosmic-ray spectrum which is not representative of the galactic average. VERITAS will measure the differences in the diffuse emission spectrum from different regions of the galaxy with excellent accuracy up to the TeV range, providing the first measurement of the cosmic-ray distribution in our galaxy at such high energies. Together with results from GLAST, a comprehensive and consistent picture of particle interactions with the ISM should evolve.

2.3 Compact Galactic Objects

Pulsar-powered nebulae: The Crab Nebula was the first detected source of VHE γ-rays (Weekes et al. 1989) and remains the standard candle for VHE observations. Unpulsed VHE emission from PSR 1706-44 (Kifune et al. 1995; Chadwick et al. 1998) and Vela (Yoshikoshi et al. 1997) suggest that plerions like the Crab Nebula may be the most prominent members of a large galactic source population. A crucial step to understanding the production mechanism of γ-rays from plerions is to determine accurately the spectrum of the VHE γ-rays. Because VHE γ-rays are at or near the end of the electromagnetic spectrum, their measurement provides some of the strongest constraints on the models. When combined with observations of the synchrotron emission spectrum, the VHE measurements can also be used to derive the nebular magnetic field. Whipple observations have now produced an accurate estimate of this spectrum for the Crab Nebula which is consistent with synchrotron-inverse Compton emission (Figure 7; Hillas et al. 1998).

With its improved sensitivity, VERITAS should be able to detect Crab-like objects anywhere within the Galaxy if their declination is $> -28°$. Its improved energy resolution and broader energy coverage will significantly improve spectral measurements leading to more accurate estimates of the nebular magnetic field and maximum electron energy and more detailed tests of γ-ray emission models. The excellent angular resolution of VERITAS may even make it possible to resolve the VHE emission region of nearby objects like the Crab Nebula.

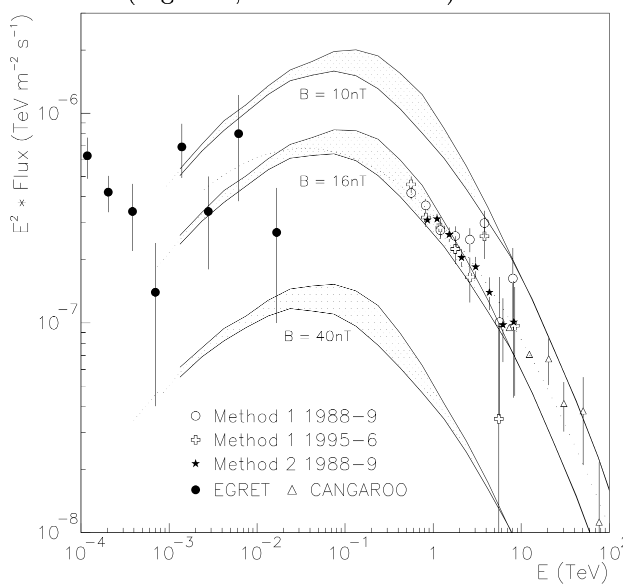

Figure 7: Crab spectrum from EGRET and VHE observations showing inverse Compton model fits for various values of the nebular magnetic field. Figure from Hillas et al. (1998).

Gamma-ray pulsars: Attenuation of γ-rays by pair-production interactions in the intense magnetic field near pulsars leads to a sharp cut-off in the spectra predicted by polar cap models. Because the outer gap models do not predict such sharp cut-offs, the detection of pulsed VHE γ-rays may be decisive in favoring the outer gap model over the polar cap model. Six pulsars are detected at EGRET energies and their high energy emission is already seriously constrained by the VHE upper limits. The excellent sensitivity and energy resolution of VERITAS should allow spectral measurements to be conducted even on these objects which are expected to have rapidly falling spectra in the VHE range. As such, VERITAS will provide detailed tests of the specific emission models.

Unidentified galactic EGRET sources: A legacy of EGRET is the 170 unidentified sources, many of which are in the Galactic plane (Hartman et al. 1999). The positional uncertainty of these sources make identifications with sources at longer wavelengths unlikely. Some of the unidentified sources which are in the galactic plane are probably SNRs and pulsars, particularly in regions of high IR density (e.g., OB associations), but some may be new types of objects. VERITAS should have the sensitivity and low energy threshold necessary to detect many of these objects. Detailed studies with the excellent source location capability of VERITAS could lead to identifications with objects at longer wavelengths. In addition, any variability in these objects would be easily identified and measured with VERITAS.

Galactic plane survey: A survey is an efficient means of observing a large sample of sources and the only way to efficiently detect new types of objects. Because of its flux sensitivity and large field of view, one of the first priorities of VERITAS will be to conduct a sensitive survey in the 100 GeV – 10 TeV energy range. To maximize the scientific returns, the first task will be to survey the region near the Galactic plane. VERITAS can observe the plane over the longitude range $0° < l < 245°$ but the initial survey will concentrate on the denser regions. For an 80-night survey of the region $0° < l < 85°$, VERITAS will be sensitive to fluxes down to ∼0.02 Crab above 300 GeV. This region encompasses 19 young, energetic pulsars, 12 unidentified EGRET sources, several X-ray binaries, and many SNRs. Thus, with this survey alone, VERITAS has the potential to significantly increase the catalog of VHE sources.

2.4 Background Infrared Radiation

In traversing intergalactic distances, γ-rays can be absorbed by photon-photon pair production on background photon fields (Gould & Schréder 1967). For VHE photons, the most important interaction is with infrared (IR) fields. Intergalactic IR photons arise from normal galaxy formation, with the spectrum and density of the IR background yielding information about the epoch and evolution of the formation process. Exotic mechanisms, such as Very Massive Objects (VMOs) or the decay of massive neutrinos, may also contribute to the IR background. Measurements of VHE spectra from extragalactic sources permit indirect investigation into the nature of the IR background field because distortions in the γ-ray spectrum due to pair-production depend on the density spectrum of the background field. VHE spectra from Mrk 421 and Mrk 501 have already been used to set upper limits on the IR background from 0.025 eV to 0.3 eV (Stecker & de Jager 1998; Dwek & Slavin 1992; Biller et al. 1998). At some wavelengths, these limits are as much as an order of magnitude below the upper limits set by the DIRBE/COBE satellite (see Figure 8). These limits place substantial restrictions on several proposed particle physics and cosmological models which would contribute to the IR background (cf., Biller et al. 1998). In particular, the contribution of VMOs to the dark matter in galactic halos must be <5% of the critical density unless dust grains substantially reprocess their radiation. In addition, the VHE results improve limits on the lifetime/branching ratio for radiative decay of heavy neutrinos in the mass range ∼0.05 eV by up to two orders of magnitude.

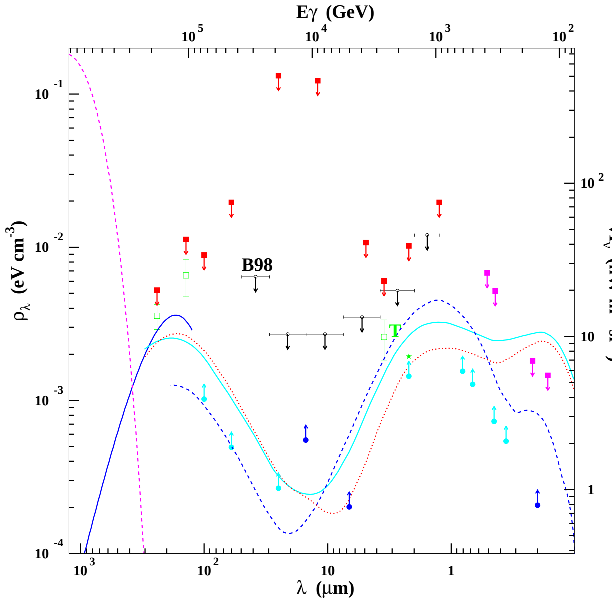

Figure 8: The diffuse intergalactic infrared background. E_γ is the energy at which the pair-production cross-section peaks for head on collisions with photons of wavelength λ. Upper limits derived from γ-ray spectra are shown as horizontal bars with arrows, marked as B98 (Biller et al. 1998). The points and the solid curve represent experimental limits or detections. The dashed line on the left is the 2.7 K cosmic microwave background and the three dashed curves are models of the IR background. Figure from Vassiliev (1999).

The current limits on the IR density are ∼5 to 10 times higher than predicted from galaxy evolution (e.g., Primack et al. 1999; Malkan & Stecker 1998). However, with better spectral measurements of existing sources and detections of more objects, particularly at higher redshift, VERITAS can substantially improve these limits, and may eventually detect the effects of the IR field.

2.5 Gamma-ray Bursts

Recent detections of X-ray and optical afterglows confirm the initial BATSE indications that at least one subset of γ-ray bursts (GRBs) have an extragalactic origin. However, the sources and mechanism for producing the GRBs remain unknown. The detection of an 18 GeV photon from a GRB more than 90 minutes after the burst was detected by BATSE (Hurley 1994) demonstrates that high energy γ-rays play an important role in the energetics of GRBs. Also, because the high energy emission can be delayed, it can be pursued with rapid follow-up observations. More recently, the Milagro Collaboration has reported a weak ($\sim 3\sigma$) detection of TeV emission from a GRB (McEnery et al. 1999) raising the possibility that TeV photons may carry a significant fraction of the energy emitted in a GRB. Because of its low energy threshold, VERITAS will be able to see bursts out to z∼1 or more. The large field of view of VERITAS (up to 10° with all telescopes pointing in slightly different regions of the sky), rapid slew speed and good angular resolution make it an excellent telescope for conducting counterpart searches. Because of the difficulty in producing

VHE γ-rays and in getting them out of the region where the burst originates, accurate measurements of a VHE component would place stringent new limits on the viable models for GRBs. In addition, the expected attenuation at high energies from interaction with background IR fields would establish the distance scale of GRBs using the high energy photons themselves.

2.6 Neutralino annihilation in the Galactic center

Current astrophysical data indicate the need for a cold dark matter component with $\Omega \approx 0.3$ (see Gawiser & Silk 1998; Primack 1998; Kamionkowski 1998). A good candidate for this component is the neutralino, the lightest stable supersymmetric particle. If neutralinos do comprise the dark matter and are concentrated near the center of our galaxy, their direct annihilation to γ-rays should produce a unique signal not easily mimicked by other astrophysical processes: a monoenergetic annihilation line with mean energy equal to the neutralino mass. Cosmological constraints and limits from accelerator experiments restrict the neutralino mass to the range 30 GeV - 3 TeV. Thus, VERITAS and GLAST together will allow a sensitive search over the entire allowed neutralino mass range. Recent estimates of the annihilation line flux for neutralinos at the galactic center (Bergström, Ullio & Buckley 1998) using a galactic model with central cusps in the density distribution of the dark matter halos (Navarro, Frenk & White 1996) predict a γ-ray signal which may be of sufficient intensity to be detected with VERITAS (Figure 9) and GLAST. The better sensitivity and lower energy threshold of VERITAS will be critical to covering a broad part of the allowed range of neutralino and dark matter parameters.

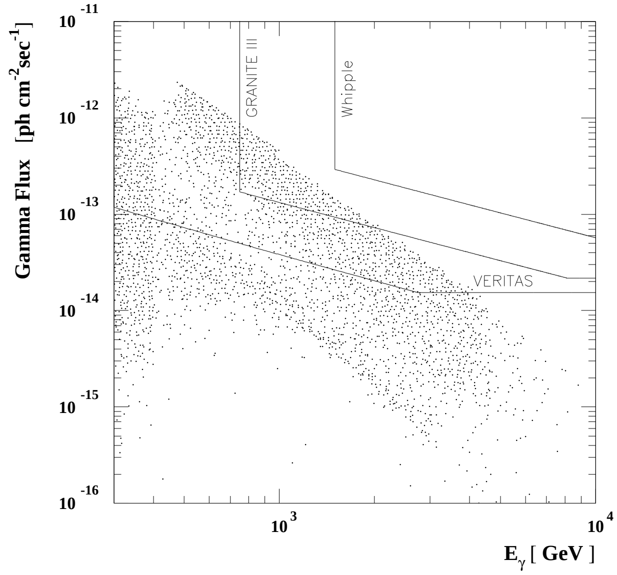

Figure 9: Neutralino annihilation rate from the Galactic center. Shown are the sensitivity curves for Whipple, the Granite III upgrade of the Whipple telescope, and VERITAS. Each point represents a particular choice of supersymmetry model parameters in the experimentally allowed range. Figure from Bergström et al. (1998).

2.7 Quantum gravity

Quantum gravity can manifest itself as an effective energy-dependence to the velocity of light in vacuum caused by propagation through a gravitational medium containing quantum fluctuations on distance scales near the Planck length ($\simeq 10^{-33}$ cm) with time-scales on the order of the Planck mass ($\simeq 10^{19}$ GeV) (e.g., Amelino-Camelia et al. 1998). Recent work within the context of string theory indicates that quantum gravity may manifest itself at a much lower energy scale than the Planck mass, perhaps as low as 10^{16} GeV (Witten 1996). TeV observations of variable emission from astrophysical objects provide a means of searching for the effects of quantum gravity. For example, the Whipple Collaboration has recently used data from a rapid flare of the AGN Mrk 421 to constrain the energy at which quantum gravity couples to electromagnetic radiation to be $> 4\times10^{16}$ GeV for some models (Biller et al. 1999). VERITAS will significantly improve short time-scale variability measurements and also will detect more distant objects. If variability on a time-scale of 1 minute is seen above 5 TeV from a source at z=0.1, VERITAS would be sensitive to quantum gravity effects within a factor of 5 of the Planck mass. In addition to AGN flares, measurements of pulsed emission from Galactic sources and of γ-ray bursts may provide avenues for investigating the effects of quantum gravity.

2.8 Primordial black holes

Low mass black holes may have been created in the early universe via gravitational collapse of inhomogeneities (Hawking 1971). These primordial black holes, if they exist, should emit a burst of radiation in the final stages of their evaporation (e.g., Page & Hawking 1976). In the standard model of particle physics, this last burst of radiation should release about 10^{30}erg in 1 s with the energy distribution peaked near 1 TeV (Halzen et al. 1991). In two years of operation VERITAS would be able to place a limit on this type of decay of 700 pc^{-3} yr^{-1}. More extreme models (e.g., Hagedorn 1968) would produce lower energy events on much shorter time-scales which may be detectable with VERITAS using a special trigger and the flash ADC system (Krennrich et al. 1999b). For these events, VERITAS would be sensitive to a level of 10^{-4} pc^{-3} yr^{-1}.

3 Technical Description

3.1 The Atmospheric Cherenkov Imaging Technique

VHE γ-ray telescopes have an inherent advantage over space telescopes because of their very large collection areas (>40,000 m^2 compared with <1 m^2). However, no anti-coincidence shield can be used in air shower detectors, so to reject the large background of cosmic rays, it is necessary to exploit the differences between the γ-ray showers and the hadronic showers which constitute the major background. The atmospheric Cherenkov imaging technique was proposed in 1977 for this purpose (Weekes & Turver 1977). The basis of the technique is the use of an array of photomultiplier tubes (PMTs) in the focal plane of a large optical reflector to record the Cherenkov image of an air shower. The geometry of the detection is shown in Figure 10.

There are basic differences in the appearance of the Cherenkov light image of a γ-ray shower (from a source centered in the field of view) and that of a typical background hadron shower coming from a random direction. The differences arise for two reasons: a) physics: the smaller transverse momentum in electromagnetic interactions compared with hadronic interactions means that the Cherenkov radiating particles in the γ-ray shower are, on average, closer to the direction of the primary; also there is no penetrating component in electromagnetic showers, so the local contribution to the light is small and the fluctuations in the shower image are far less; b) geometry: the orientation of the roughly elliptical image of a shower depends on the angle it makes with the optic axis of the telescope; a shower whose axis coincides with the optic axis (the trivial case) gives a round image that is centered on the axis; showers which are parallel to the axis but fall up to 120 m away have elliptical images whose major axis intersect the optic axis; this holds true for γ-ray and hadron showers but it is easier to characterize the axis of a γ-ray shower since its image is more compact.

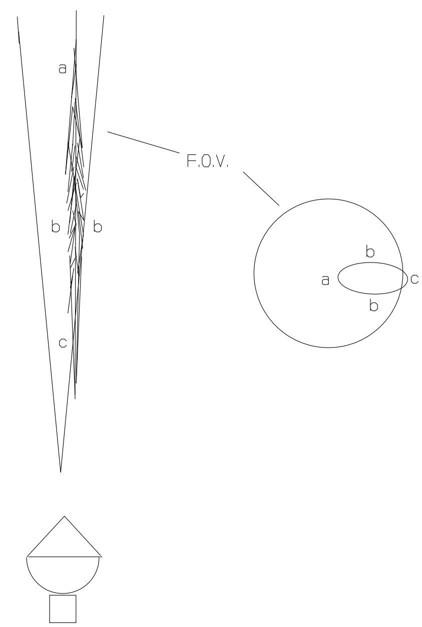

Figure 10: The imaging technique. The cone of acceptance of the camera intercepts the core of the air shower. The elliptical contour of a typical Cherenkov light image as seen in the focal plane of the Whipple Observatory camera (diameter 3.5°) is shown on the right. Images of γ-ray showers coming from a source parallel to the optic axis are narrow and point towards the center. Images from background cosmic rays are broader and have no preferred pointing direction.

The power of the imaging technique was demonstrated using an array of photomultiplier tubes (PMTs) in the focal plane of the Whipple Observatory 10 m optical reflector; the detection of the Crab Nebula was the first major success of the technique (Weekes et al. 1989; Vacanti et al. 1991). The background was rejected with 99.7% efficiency and the source location was accurate to 0.05°.

3.2 VERITAS Telescope Design

The seven telescopes in VERITAS will be identical and will have the geometrical layout shown in Figure 11. Six telescopes will be located at the corners of a hexagon of side 80 m and one will be located at the center.

The telescopes will each have a camera consisting of 499 pixels with a field of view of 3.5° diameter. The design of the individual telescopes will be similar to that of the existing Whipple 10 m reflector which has proven to be an excellent facility for VHE γ-ray astrophysics. It has withstood mountain conditions for over thirty years, has good optical quality, a structure sufficiently rigid that flexure is negligible at all elevation angles, and it has good UV reflectivity.

The Davies-Cotton optical design (Davies & Cotton 1957) used in the 10 m reflector (and many subsequent γ-ray telescopes) has facet mirrors which are spherical and identical, facilitating fabrication at a reasonable cost and making alignment easy. It also has smaller off-axis aberrations than a parabolic reflector so that it has good image quality out to a few degrees from the optic axis. Its one limitation, that the surface is not isochronous, means that the 10 m reflector introduces a time-spread of 6 ns into the light pulse. We, as well as other research groups, have investigated alternative designs but conclude that the Davies-Cotton collector provides the optimal combination of optical quality and cost effectiveness. Increasing the f-number from $f/0.7$ to $f/1.2$ substantially improves the optical quality of the telescope (Figure 12). It is then possible to match the inherent fluctuations in the shower images with a camera that has a reasonable number of pixels ($\approx$ 500) and appropriate field of view ($\approx$3.5°).

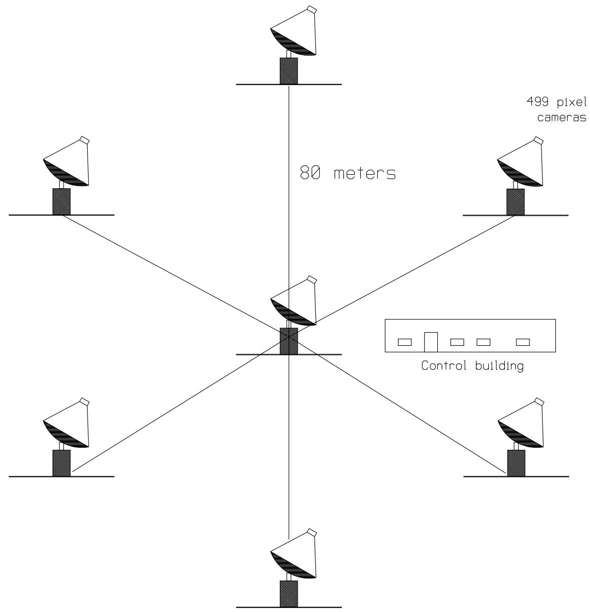

Figure 11: Layout of telescopes in VERITAS.

The desirable optical parameters of the telescope follow from the characteristics of a γ-ray shower Cherenkov image. For a γ-ray source at the center of the field of view (FoV), the average image centroid (distance) is at about 0.85° from the center of the focal surface, and moves to slightly larger values at larger energies. The image has a r.m.s. width and length of about 0.14° and 0.25°, respectively. The reflector will have sufficient resolution to record structure on this scale. The intrinsic time width of the Cherenkov light is a few nanoseconds and the spread in light across the $f/1.2$ reflector is 3-4 ns.

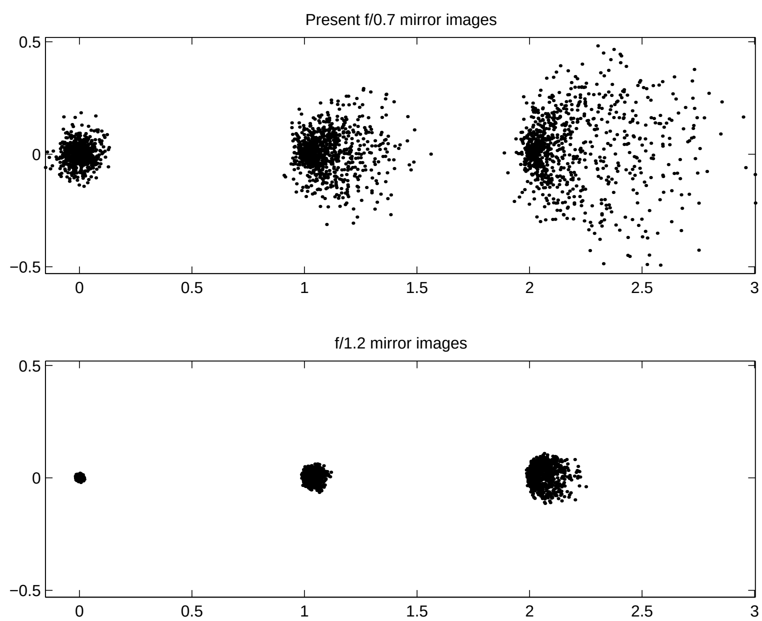

Figure 12: Davies-Cotton images at 0°, 1°, and 2° for f/numbers of 0.7 (like the present Whipple telescope) and 1.2 (proposed for VERITAS). The facet size is 60 cm and the image size is given in degrees. A total of 1000 points lie in each image.

A key factor in the reflector quality and cost is the mirror facets. Although a number of mirror materials and fabrication technologies have been developed and investigated for this project, a conventional approach has been chosen as the most cost effective. The facets will be made of float glass, slumped and possibly polished, aluminized and anodized. They will be hexagonal in shape to permit close packing and will be 60 cm across the flats.

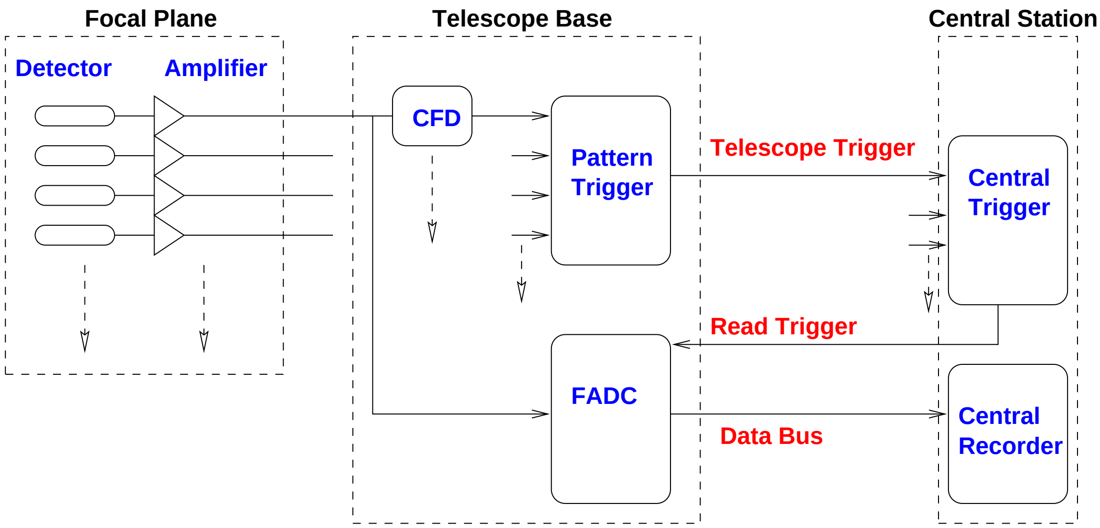

Figure 13: Outline of electronics.

3.3 Mounts: Optical Support Structure/Positioner

The VERITAS telescopes will be based on the same design as the Whipple 10 m optical reflector but will have some significant differences. A range of possible variations in the initial specifications of critical parameters (aperture, f/number, wind loading, storm survival, stiffness, etc.) were evaluated by the engineering firm, Simpson, Gumpertz and Heger (SG&H). This firm was also responsible for the design and construction of the current 10 m telescope. On the basis of their study, it was determined that an OSS of trussed steel of 10 m aperture and 12 m focal length ($f/1.2$) could be designed to match commercially available positioners. They confirmed that a telescope with $f/1.2$ optics can be constructed locally from standard materials to meet our final design specifications. Mirror alignment accuracy can be held to an angular accuracy of 0.01°. Effects due to gravitational slumping during slewing will be less than 2.2 mm on the camera face; wind distortions will be less than 2 mm up to 30 m.p.h.. Slew speed can be as high as 1° per second on both axes. The total weight of the OSS, mirrors, counterweights and the detector is estimated to be 35,000 lb. Commercially available positioners from radio and radar antenna manufacturers, e.g., from Scientific-Atlanta, Vertex or RSI can meet the required specifications.

3.4 Electronic Camera

3.4.1 Outline

The electronic camera for each VERITAS telescope is similar to previous imaging atmospheric Cherenkov detectors (Cawley et al. 1990) but with some significant improvements. An outline of the components of the camera is shown in Figure 13. The focal plane detector consists of an array of 499 separate PMTs. The signals are first amplified near the detectors in the focal plane and then transmitted to the local electronics located near the telescope base. These systems provide the local trigger and convert the analog signals to digital form. To take full advantage of the fast Cherenkov pulse structure, the split signals from the individual PMTs are fed to fast constant fraction discriminators (CFDs) to provide the signals necessary to form the initial trigger by detecting coincidences on a time-scale $<$15 ns. The outputs from these discriminators are fed to a local pattern trigger unit which tests for adjacent detector hits in the telescope. The pattern trigger signal is sent to the central trigger location where programmable delays are applied to the trigger signal from each telescope to correct for the difference in the time of arrival of the Cherenkov wavefront at the individual telescopes due to the source location in the sky. An array trigger can be formed from a combination of individual telescope triggers at the central trigger. The trigger is designed to record all γ-ray events that contain enough light to be usefully identified as γ-ray events (reconstruction threshold) while limiting the trigger rate to a manageable level.

The other branch of the analog signal from each detector is fed to a flash analog to digital converter (FADC) which digitizes the detector waveform into a circulating memory. This results in a digitized version of the signal pulse from each detector. When a readout trigger decision has been made for an individual telescope, a sub-array of telescopes or the full array, the associated electronics loads the appropriate section of the FADC memory of those signal channels with hits to a data bus which is read out by a controller and stored in reflective memory modules. This information is read out by local CPUs and merged into event data for the telescope. The individual telescope data is transmitted the central station, merged with data from the other telescopes and stored. A centrally generated optical pulse is used to synchronize individual electronic channels and the time tagging of events across the array.

Some of the individual elements of the VERITAS electronic cameras are discussed briefly here.

3.4.2 Front-end Electronics

Photomultiplier Tubes: A low noise, high gain ($> 10^6$), photon counting detector, with fast time response (risetimes $<$ a few ns) matched to the intrinsic temporal width of the γ-ray induced air shower is necessary to increase the signal-to-noise ratio and to operate VERITAS at the lowest possible energy threshold. These requirements are presently satisfied only by PMTs and 25 years of experience with these devices leads us to base the VERITAS system upon them. The focal plane will contain 499 hexagonally packed PMTs providing an effective FoV of $\sim 3.5°$. The spacing between the PMTs corresponds to a focal plane angular distance of 0.15°. The active light collection diameter of the PMTs is 25 mm. The collection efficiency is increased by the use of Winston light concentrators. Tests have identified the Hamamatsu R7056, with a bialkali photocathode and a UV glass window, as one PMT which satisfies our requirements.

High Voltage Supply: We plan to use a modular commercial high voltage supply where each PMT has a separately programmable high voltage. These are used to adjust the PMT gains and to reduce the current draw when a bright star image falls directly on a specific PMT. The high voltage is supplied by cables attached to each PMT from a system crate which is carried on each telescope. Commands to each telescope system are sent from the central station.

Signal Amplifiers: A custom circuit with a linear amplifier is attached to each PMT in the focus box. This circuit is based on a standard integrated circuit amplifier chip, e.g., Analog Devices AD8009, which has a bandwidth of 1 GHz. The targeted gain of the PMT and amplifier provides a signal level of ~2 mV/photoelectron.

Cabling: Cabling from the focal plane PMTs to the telescope electronics is through standard RG58 coaxial cable (as used in the current 10 m telescope). This method introduces some time dispersion into the signals. An analog optical fiber system with sufficient dynamic range (1:1000) is presently under development and is being tested on the Whipple 10 m telescope. Fibers introduce no dispersion and are light-weight. If these tests are satisfactory optical fibers will be an attractive upgrade to coaxial cabling and will permit much of the electronics to be located in the central control building.

3.4.3 Trigger Electronics

Constant Fraction Discriminators: Constant Fraction Discriminators (CFDs) are incorporated into a custom CFD/scaler module which also measures the discriminator firing rates on each channel. The analog bandwidth of this system is > 500 MHz. The discriminator threshold is programmable by command. This module also has a short adjustable delay element to allow the timing in each channel to be matched at the 1 ns level. An analog fanout of the PMT signal is provided from this board to the FADC system.

Trigger Levels: For practical operation, VERITAS must trigger at a rate $\leq$1 kHz. A higher rate produces unacceptable dead-time in the acquisition systems. To facilitate this rate, while keeping the energy threshold of the detector at a minimum, a trigger scheme of four levels has been developed. The levels are defined as:

Level 1 Each PMT is connected to a discriminator which has a programmable threshold. The night-sky background light produces rates (singles) given by the dotted curve in Figure 14. At low thresholds the dominant contribution to the trigger rate comes from fluctuations in the number of single photoelectrons (p.e.) produced by night-sky light. At higher thresholds the background rate is dominated by PMT afterpulsing. At a threshold of 4.2 p.e., the Level 1 trigger rate is ~1 MHz for each channel.

Level 2 A hardware pattern trigger at each telescope based on Level 1 triggers can reduce the background by discriminating between photon-initiated showers images, which are compact, and background triggers caused by sky noise or afterpulsing, which have random locations in the camera plane. The dashed curve in Figure 14 shows the expected rate of these background events when the pattern requirement is that the 3 nearest neighbors in the 499 pixel camera are hit. The Pattern Trigger will likely follow the scheme presently being used at the Whipple Telescope.

Level 3 The central station receives the Level 2 triggers from each telescope. The Level 3 trigger system selectively delays each Level 2 signal to account for the wavefront orientation and determines if the overall array trigger condition is satisfied. The trigger condition will depend on the array configuration and the observing strategy, but will typically require the time coincidence of several telescopes. The solid curve in Figure 14 shows the expected background rates for this trigger if 3 of 7 telescopes fire within 40 ns coincidence time. If the Level 3 trigger condition is met, readout of the telescope event information will be initiated.

Level 4 The background trigger rate can be reduced by demanding that the individual telescope trigger clusters conform to the predicted parallactic displacement of the γ-ray images. Thus, a high level trigger, implemented either in hardware or in software, can be used to significantly suppress the hadronic background. This system is currently in the development stage.

3.4.4 Signal Recording

Flash ADCs: A FADC provides a digitized version of the Cherenkov pulse waveform, giving the maximum information possible about the shape and time structure. These devices allow operation of the individual telescopes well into the night sky background, eliminate the need for delay cables (minimizing signal dispersion), and allow real-time calibration of the PMT and signal cable propagation times. Also, the time structure of the pulse is expected to become wider near the edge of the Cherenkov light pool, and with the FADCs these effects can be corrected for in later analysis of the digitized pulses. The increasing availability of high bandwidth FADC chips for commercial purposes makes it possible to include a FADC in every detector channel of VERITAS. However commercial modules are expensive and we plan to custom build our own units. A prototype FADC system has been developed and tested on the Whipple telescope and appears to have all the necessary parameters for VERITAS. Each FADC channel uses a commercially available 8-bit FADC integrated circuit. This system has a sample rate of 500 MHz and a bilinear range of 0 to 630 (1260) p.e., with a gain of 4 (2) digital counts per p.e. Using the time over threshold of the digitized Cherenkov pulse can significantly extend the range and studies to determine the utility of this technique are in progress.

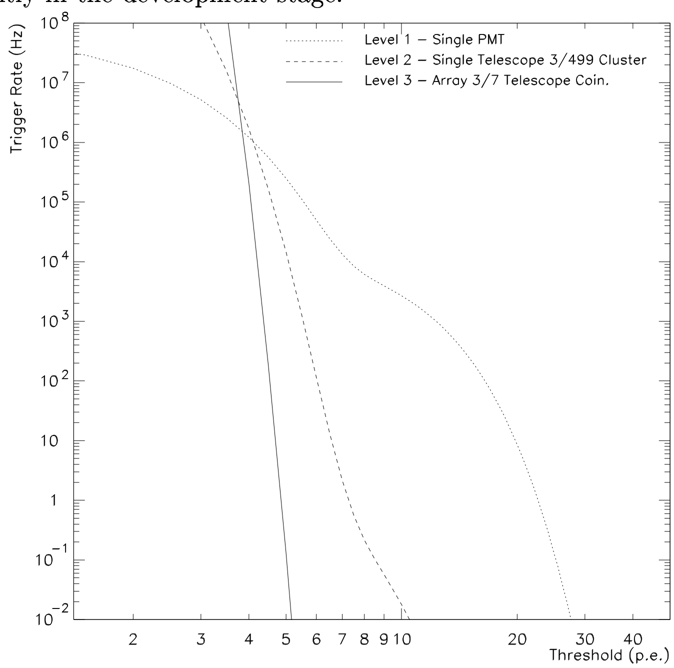

Figure 14: Expected rates from VERITAS. The various curves are discussed in the text.

Data Acquisition: The telescope electronics are based largely around the VME standard electronic architecture: a fast VME backplane and distributed computation performed by local CPUs running a real-time operating system. Each controller will be connected, using fast, fiber-optic connections to a local workstation which in turn is connected to a central high speed switch connected to the central CPU. The central CPU will perform control and quicklook functions, further data compression and integration of the distributed data. This system will operate using cyclic and multi-thread processes, adhering to POSIX standards where possible in order to maintain future systems compatibility. Secondary systems to control mount movement and high voltage generation will be inexpensive Pentium PCs running a UNIX-like operating system such as LINUX. Again, communication will be via Ethernet connection. For a telescope readout rate of ~1 kHz each telescope is expected to have an average data flow rate of ~800 kbyte/s, resulting in a 200 kbyte/s rate on any VME backplane. This rate includes real Cherenkov events and spurious background hits. The VERITAS data acquisition system expects to operate well within this limiting range.

4 Array performance

Extensive simulation studies have been used to determine the optimum configuration for VERITAS and to characterize its performance. The VERITAS design is optimized for maximum sensitivity to point sources in the energy range 100 GeV - 10 TeV, but with significant sensitivity in the range 50 GeV - 100 GeV and from 10 TeV - 50 TeV. Also, the chosen field of view (3.5°) is large enough to conduct an efficient sky survey and study extended sources while maintaining a fine pixellation of the camera for a low energy threshold. Here we give a brief justification for the chosen configuration and concentrate on describing its capabilities.

The baseline configuration for VERITAS is described in § 3. The performance characteristics of this configuration are outlined in Table 1. The performance characteristics listed are for a telescope trigger requiring 3 adjacent PMTs to record more than 4.2 photoelectrons (p.e.) within 14 ns (see §3 for details on telescope triggering). The 4.2 p.e. trigger threshold level is set by the sustainable single telescope trigger rate at which VERITAS can operate (1 MHz) and by the requirement that the trigger rate from fluctuations of the night sky background (NSB) not exceed 10% of the total cosmic-ray rate of 1 kHz. We emphasize that our definition of the energy threshold is the point where the rate of γ-rays per unit energy interval from the Crab Nebula is highest. This definition is quite conservative because VERITAS has good sensitivity to γ-rays at energies well below this (see Figure 17).

Table 1: Performance of VERITAS

Characteristic	E	Value
Energy threshold[a]		75 GeV
Flux sensitivity[b]	>100 GeV	9.1×10^{-12}cm^{-2}s^{-1}/15 mCrab
	>300 GeV	8.0×10^{-13}cm^{-2}s^{-1}/5 mCrab
	>1 TeV	1.3×10^{-13}cm^{-2}s^{-1}/7 mCrab
Angular resolution	50 GeV	0.14°
	100 GeV	0.09°
	300 GeV	0.05°
	1 TeV	0.03°
Effective area	50 GeV	1.0×10^{3}m^{2}
	100 GeV	1.0×10^{4}m^{2}
	300 GeV	4.0×10^{4}m^{2}
	1 TeV	1.0×10^{5}m^{2}
Crab Nebula	>100 GeV	50/minute
γ-ray rates	>300 GeV	7/minute
	>1 TeV	1/minute
Energy resolution[c]		<15%

[a]Energy at which the rate of photons per unit energy interval from the Crab Nebula is highest for a 4.2 photoelectron trigger threshold.
[b]Minimum integral flux for a 5σ excess (or ≥10 events) in 50 hours of observations of a source with a Crab-like spectrum.
[c]RMS $\Delta E/E$

4.1 Justification of VERITAS parameters

To investigate the optimum array configuration, several parameters were varied: the number of telescopes, the spacing between the telescopes, the focal length of the telescope, the aperture of the telescopes, and the field of view of the cameras. The number of channels in the camera was fixed before the optimization for cost reasons. Thus, our investigations of different camera fields of view are simultaneously investigations of changes in the spacing of the PMTs. In the central energy range of 200 GeV to 1 TeV, the sensitivity of the array to point sources is not significantly affected by small changes in the array's characteristics. Thus, the choices of telescope parameters are driven mostly by their effects on the performance of VERITAS at the low and high ends of its sensitive energy range.

We have chosen the stereoscopic route to advance the atmospheric Cherenkov technique due to its excellent angular resolution and background rejection. At a minimum, three telescopes are necessary to utilize the stereoscopic imaging technique. Two telescopes can be used for bright images, but faint cascades can only be accurately reconstructed with images in three telescopes because the individual image axes are not well-defined. There are three primary reasons for choosing a seven telescope array over one with three to four telescopes. First, a seven telescope array is significantly more flexible because it can be split into sub-arrays halving the time required for surveys, making it possible to more effectively monitor variable AGN and to more efficiently participate in correlated observational campaigns, e.g., with GLAST, X-ray telescopes and other Cherenkov telescopes. Previous multiwavelength campaigns with the Whipple telescope have been highly successful in probing physical mechanisms in AGN. Second, when used as a single instrument, a seven telescope array better measures spectra over a broad energy range due to larger collection area and sensitivity at low energies. Determination of accurate spectra over broad energy ranges bears directly upon models of γ-ray production mechanisms for SNR, AGN and perhaps models of intergalactic background radiation. Finally, some cosmic sources (e.g., γ-ray pulsars or γ-ray bursts) may be detectable only in the lowest energy range which is accessible only with the full seven-telescope array.

The separation between the telescopes was chosen to be 80 m. This provides the best combination of flux sensitivity and energy threshold. Increasing the spacing does not improve flux sensitivity in the 200 GeV - 1 TeV energy range but it does increase the energy threshold. Decreasing the spacing can reduce the energy threshold somewhat, but the sensitivity is significantly impaired over the entire energy range because the stereoscopic capabilities become less efficient and the effective area of the array decreases.

The chosen focal length for the telescopes is 12 m, making this an $f/1.2$ system. Increasing the focal length from the current $f/0.7$ system significantly improves the optical quality of the telescopes by reducing the effects of aberrations (see § 3). This improvement is necessary to match the angular size of the PMTs in the VERITAS cameras ($\sim 0.15°$). However, increasing the focal length beyond 12 m does not improve the performance of VERITAS enough to justify the increased cost and complexity needed to achieve the required alignment precision and stability for the pixel size chosen. Also, the reduction in energy threshold for increasing the focal length beyond 12 m is outweighed by the less efficient light collection caused by increasing the pixel separation to maintain the required field of view. Thus, 12 m provides the best combination of improved optical quality, sufficient field of view and small pixel spacing.

The chosen field of view of the telescope is 3.5°. From experience operating the Whipple telescope, this field of view is required for individual telescopes to accurately reconstruct images from point sources and it also gives significant sensitivity to off-axis or extended sources. Increasing the field of view beyond this will improve the high energy response of the telescope, but also increases the energy threshold for the fixed number of channels. The chosen field of view is a compromise between these competing priorities.

4.2 Angular resolution

We define the angular resolution as the width of a two-dimensional Gaussian fit to the distribution of reconstructed directions for individual photons from a point source. The angular resolution of VERITAS as a function of energy threshold is shown in Figure 15. VERITAS will have better angular resolution than any existing detector (in space or on the ground) operating above a few MeV. The main reason for the excellent angular resolution of VERITAS is its stereoscopic imaging capability. For a single telescope, the photon arrival direction is well-defined only in the direction perpendicular to the axis of the image, though the direction parallel to the direction of the image axis can be roughly estimated (Buckley et al. 1998). Multiple sampling of the shower from the VERITAS telescopes overcomes this difficulty and, for larger showers, can average out fluctuations. The angular resolution alone leads to better background

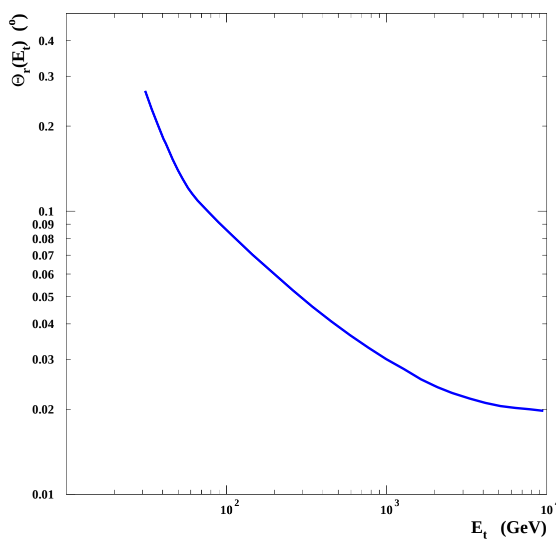

Figure 15: Angular resolution of VERITAS as a function of array energy threshold.

rejection than existing single telescopes and it also will allow the emission regions of extended sources to be mapped to arcminute accuracy.

4.3 Collection area

The collection area of the array reflects a combination of the area over which the array can detect γ-ray showers and the efficiency for retaining those events after analysis. The effective area of VERITAS as a function of photon energy is shown in Figure 16 for the estimated trigger threshold of 4.2 p.e. at which VERITAS will operate. For comparison, the effective area of the Whipple telescope near 1 TeV is approximately 4×10^4 m^2 (Hillas 1996). The effective collection area at low energies is reduced because these showers emit fewer Cherenkov photons and so must arrive with optimum geometry to trigger the telescope and allow for event reconstruction. For the highest energies, the collection area levels out because the limited FoV of the telescope truncates these images which develop low in the atmosphere.

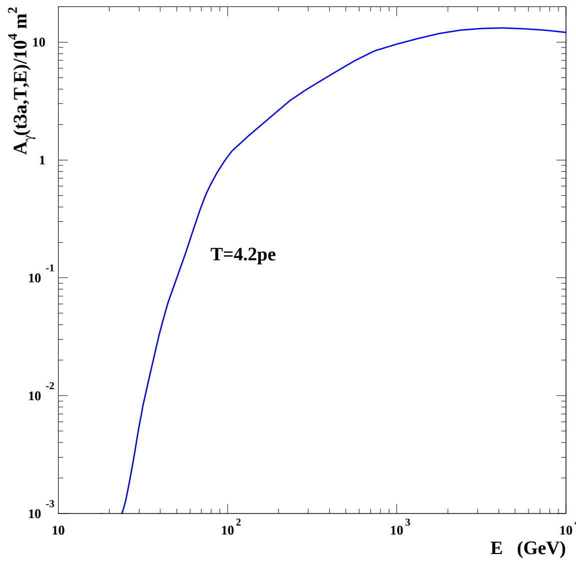

Figure 16: The collection area of VERITAS as a function of photon energy.

4.4 Energy threshold

We define the energy threshold of VERITAS as the energy at which the differential rate of *reconstructed* γ-rays from the Crab Nebula per unit interval of energy reaches its maximum. Reconstructed γ-rays are those whose images pass an image cleaning procedure (to eliminate pixels whose light is dominated by fluctuations of the NSB light), a reconstructed direction cut, and an image shape cut. **This rate curve is shown in Figure 17 for a 4.2 p.e. pixel trigger threshold and indicates an energy threshold of approximately 75 GeV.** This threshold is somewhat higher than the *trigger* energy threshold, which is the peak in the γ-ray rate for events triggering the telescope, because low energy Cherenkov events which trigger the telescope often do not produce enough light to be used in the analysis. However, events at energies below the array threshold which trigger the array can still be successfully reconstructed, as shown by the extent of the rate curves below the peak. Thus, objects with spectral cut-offs below the array energy threshold may still be detectable.

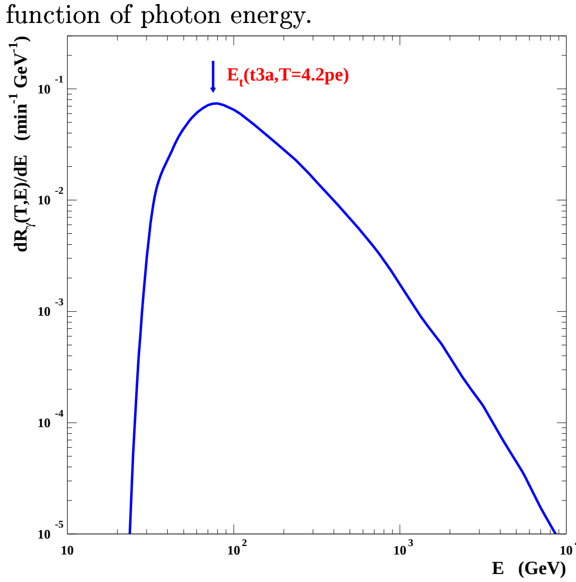

Figure 17: Differential detection rates of the Crab Nebula for VERITAS. The peak of the curve gives the array energy threshold.

An energy threshold of 75 GeV is a factor of 4 lower than that reached by existing imaging Cherenkov telescopes. This improvement comes from the combination of stereoscopic reconstruction of events, which permits effective background rejection at lower light levels than a single telescope, and the multi-telescope trigger, which permits the operation of the individual telescopes much further into the region where fluctuations in the NSB dominates the telescope trigger rate.

4.5 Energy resolution

The energy resolution of VERITAS will be considerably better than that of the Whipple telescope for three reasons: (1) the shower core location will be known, (2) several telescopes will view each event at different distances from the shower core, and (3) each camera will have finer pixellation (0.15° vs. 0.25°). The location of the core of the shower will be estimated with an accuracy of about 10 m. With a single telescope, the core distance can be estimated using the location of the image centroid relative to the source position, but the correlation is not very tight and the corresponding energy estimate is not very accurate. For the Whipple telescope, the RMS energy resolution using this technique is $\Delta E/E \approx 0.35$ (Mohanty et al. 1998).

For our estimate of energy resolution for VERITAS, we used simulated showers from γ-rays with energies >200 GeV whose arrival direction was reconstructed to within 0.1° of the source position. We also required that each telescope record >20 p.e., after image cleaning, to avoid images significantly contaminated by NSB fluctuations. The reconstructed energy for an individual telescope is a function of the amount of light in the shower, the distance of the telescope from the shower core, and the location of the image centroid relative to the source position. With the core location known, the centroid location gives information about the height of emission detected by the telescope, further improving the resolution compared to a single telescope. The final energy estimate for the array is the average from individual telescopes which detected at least 20 p.e.

The resulting overall energy RMS resolution is $\Delta\mathrm{E}/\mathrm{E} \approx 0.10 - 0.15$ from 0.2 to 10 TeV. The resolution improves slowly as the energy of the shower increases. Below 200 GeV, the energy resolution degrades somewhat, but not significantly. This resolution will likely be improved through more sophisticated energy estimates and through the use of more restrictive cuts on events used in the energy analysis.

4.6 Flux sensitivity

The performance of VERITAS is summarized by its flux sensitivity versus energy. The minimum detectable flux of γ-rays is defined by the confidence level required for detection or the statistics of the detected photons. We require a 5σ excess of γ-rays above the background, or 10 photons (below this, Poisson statistics must be used). We estimate the flux sensitivity for 50 hours of observations on an object with a spectrum given by $\mathrm{dN/dE} \propto \mathrm{E}^{-2.5}$, as seen from the Crab Nebula in this energy range. We apply direction and image shape cuts to reject background events.

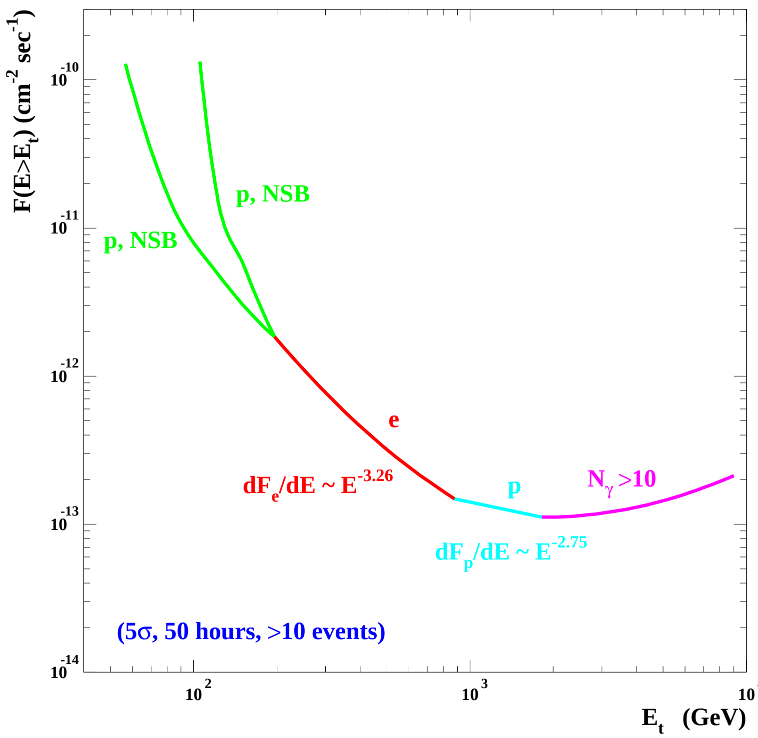

Figure 18: The sensitivity of VERITAS to point-like sources in 50 hours of observing. The dominant background as a function of energy threshold is indicated (see text for details). The two curves at low energies indicate the sensitivity of VERITAS in dark (lower curve) and bright (upper curve) NSB regions.

The γ-ray flux sensitivity of VERITAS for point sources as a function of array energy threshold is shown in Figure 18. The complex shape of the sensitivity curve is caused by different energy regions being dominated by the different backgrounds shown in Figure 18. For energies above 2 – 3 TeV, the sensitivity of VERITAS is limited by photon statistics. Larger telescope fields of view can improve this sensitivity in the future, as can large zenith angle observations. In the region near 1 TeV, the sensitivity is limited by those rare cosmic-ray protons which mimic γ-rays by converting most of their energy into an electromagnetic cascade in the first few interactions (prompt decay of π^0). In the energy region between 200 GeV and ~1 TeV, the background rejection of VERITAS is so good that diffuse cosmic-ray electrons are the dominant background instead of hadronic cosmic rays. The region below 200 GeV is limited by hadronic cosmic-ray events whose reconstruction is significantly affected by small fluctuations in the NSB. The more sensitive of the two curves indicates a relatively dark observation region (like an AGN with no bright stars in the FoV) while the less sensitive curve indicates a region where the NSB light is approximately 4 times brighter (as in some regions of the Galactic plane).

5 Status of VHE Gamma Ray Astronomy

5.1 Background

In 1968, the Whipple Observatory 10 m optical reflector was put into operation for ground-based studies of VHE γ-ray sources; between 1968 and 1978 the Smithsonian group was active in developing atmospheric Cherenkov detectors to detect γ-rays in the TeV energy range. The Whipple Gamma-Ray Collaboration was formed in 1982 to exploit the potential of the imaging technique. The Whipple Gamma-Ray Collaboration has recently completed its GRANITE III upgrade in which the 109 pixel camera (used in the initial detections of the Crab Nebula, Markarian 421 and Markarian 501) has been replaced by a wide field 331 pixel camera (in 1997) and a high resolution, 490 pixel, camera (in 1999).

5.2 Status

In recent years VHE γ-ray astronomy has seen significant advances in technique (Ong 1998;Catanese & Weekes 1999). There are nine groups now using the Cherenkov imaging technique (e.g., CAT, Barrau et al. 1998; CANGAROO, Hara et al. 1993; HEGRA, Konopelko et al. 1999; 7TA, Aiso et al. 1997). These techniques are relatively mature and the results from observations, with different telescopes, of the same source at the same time are consistent (Protheroe et al. 1997). Vigorous observing programs are now in place at all of these facilities. An important milestone for the field has been reached in that both galactic and extragalactic sources have been reliably detected (Weekes 1999).

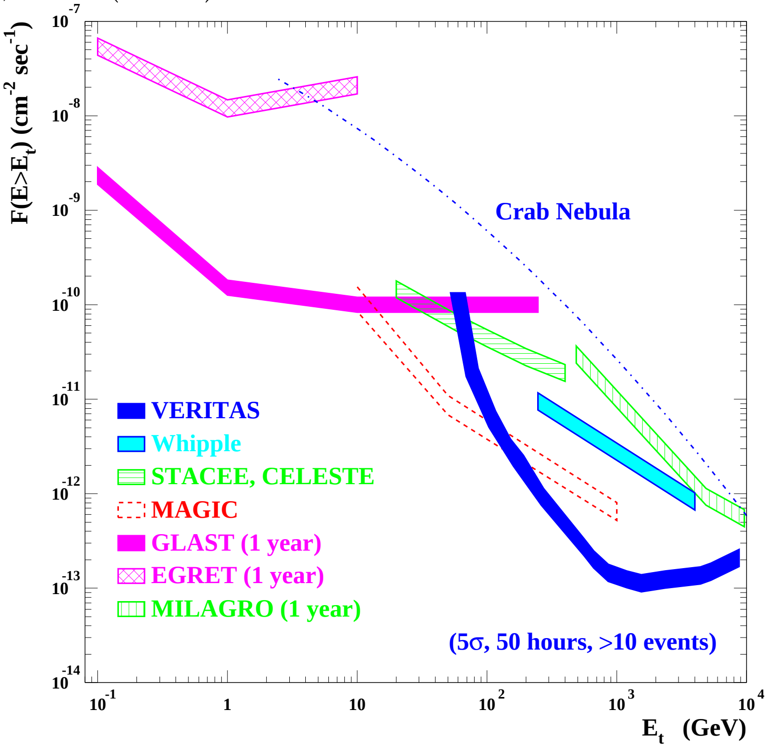

Figure 19: Comparison of the point source sensitivity of VERITAS to Whipple (Weekes et al. 1989), MAGIC (Barrio et al. 1998), CELESTE/STACEE (Quebert et al. 1995; Chantell et al. 1998); GLAST (Gehrels & Michelson 1999), EGRET (Thompson et al. 1993), and MILAGRO (Sinnis et al. 1995). The sensitivity of MAGIC is based on the availability of new technologies, e.g., high quantum efficiency PMTs, not assumed in the other experiments. EGRET, GLAST and MILAGRO are wide field instruments and therefore ideally suited for all sky surveys. The turn-up in the VERITAS sensitivity at higher energies is primarily caused by the limited field of view of the cameras and the requirement that VERITAS detect at least 10 photons.

To fully exploit the potential of ground-based γ-ray astronomy the detection techniques must be improved. This will happen by extending the energy coverage of the technique and by increasing its flux sensitivity. Ideally one would like to do both but in practice there must be trade-offs. Reduced energy threshold can be achieved by the use of larger, but cruder, mirrors and this approach is currently being exploited using existing arrays of solar heliostats (STACEE (Chantell et al. 1998) and CELESTE (Giebels et al. 1998)). A German-Spanish project (MAGIC) (Barrio et al. 1998) to build a 17 m aperture telescope has also been proposed. These projects may achieve thresholds as low as 20-30 GeV where they will effectively fill the current gap in the γ-ray spectrum from 20 to 200 GeV but with poor energy resolution and small fields of view. Ultimately this gap will be covered by GLAST with weaker point source sensitivity at the higher energies. This next generation γ-ray space telescope is scheduled for launch in 2005 by an international collaboration (Gehrels & Michelson 1999). Extension to higher energies (>10 TeV) can be achieved by atmospheric Cherenkov telescopes working at large zenith angles and by particle arrays at very high altitudes. The MILAGRO water Cherenkov detector in

New Mexico (Sinnis et al. 1995) operates 24 hours a day with a large field of view and has good sensitivity to γ-ray bursts and transients.

The primary objective of VERITAS will be to have high sensitivity in the 100 GeV to 10 TeV range. The German-French HESS (initially four and eventually perhaps sixteen 12 m class telescopes) will be built in Namibia (Konopelko 1999) and the Japanese CANGAROO-IV array (with four telescopes in Australia) (Matsubara 1997) will have similar objectives for observations in the southern hemisphere. MAGIC, HESS and CANGAROO are approved projects with target completion dates in 2001 to 2004. The arrays will exploit the high sensitivity of the atmospheric Cherenkov imaging technique and the high selectivity of the array approach. The relative flux sensitivities as a function of energy are shown in Figure 19, where the sensitivities of the wide field detectors are for one year and the ACT are for 50 hours; in all cases a $5\,\sigma$ point source detection is required. The VERITAS sensitivity is taken from §4 (cf., Figure 18).

It is apparent from this figure that, on the low energy side, VERITAS will complement the GLAST mission and will overlap with STACEE and CELESTE. At its highest energy it will overlap with the Tibet Air Shower Array (Amenomori et al. 1997). It will cover the same energy range as MILAGRO but with greater flux sensitivity. As a northern hemisphere telescope VERITAS will complement the coverage of neutrino sources to be discovered by AMANDA and ICE CUBE at the South Pole.

6 Management

6.1 Management Structure

The VERITAS project will require a formal administrative structure with Teaming Agreements between the various institutions; a draft agreement has been circulated amongst the institutions. The administrative structure common to such large projects will be adopted. The main components are the VERITAS Executive Committee (VEC), the Project Office and the Sub-Projects. The respective responsibilities of these components are described below.

6.2 VERITAS Executive Committee

The VEC, with the assistance of the Project Manager and Project Scientist, will be responsible for the following tasks:

- Providing scientific leadership to the project
- Determining the membership of the collaboration
- Drawing up the overall project plan and yearly plans
- Outlining the technical work to be pursued during that year
- Determining the availability of resources to accomplish the proposed work
- Assigning detailed responsibility for carrying out such work, thereby defining sub-project teams, team leaders and updating the List of Sub-Projects as necessary
- Selection of successors to the Project Scientist and Project Manager, when necessary, in agreement with the Director of SAO.

Each major contributing institution will appoint one member to the VEC, to serve for three years. At the beginning of each calendar year, the VEC will elect one of their members to act as Chair for the year. Membership of the Collaboration may be modified, with a two-thirds (2/3) vote of the VEC. Other decisions of the VEC will be decided by simple majority; in the event of a tie the Chair shall have the deciding vote. The Project Scientist and Project Manager will be non-voting members of the VEC (except when they also serve as representatives of Collaboration groups).

6.2.1 Project Office

The Project Office, under the direction of the VEC, will be responsible for the following tasks:

- Providing local scientific leadership and providing the day-to-day management of the project
- Drawing up the overall project specifications, project plan and yearly plans for approval
- Assessing the work accomplished to date; monitoring progress at frequent intervals
- Outlining the technical work to be pursued during that year and estimating the cost of such work

- Determining the availability of resources to accomplish the proposed work
- Assigning detailed responsibility for carrying out the tasks, monitoring the tasks and ensuring that they are within agreed schedule and budget
- Monitoring the task interfaces.

To aid the Project Office, each institution will provide to it timely reports specifying in some detail both past expenditures and future plans regarding finances and personnel. These reports will be due to the Project Office one year from the signing of this agreement, and yearly thereafter. The Project Office will issue its report within 60 days after the end of each year's activities.

The Project Office will be located at the VERITAS site 40 miles south of Tucson, Arizona. The Project Office will avail of the general administrative services of the Whipple Observatory Administrative Office nearby. The Project Office will consist of the following positions.

Project Scientist: The Project Scientist will report directly to the VEC and will be responsible for ensuring that their policies are adhered to and their instructions are carried out. He/she will be responsible for the Project Office and will act as Spokesperson for the project.

Project Manager: The Project Manager will report to the Project Scientist and will manage the Project Office. He/she will provide project management for the total project. He/she will monitor all Sub-projects and assist in their fiscal planning and scheduling; problems (fiscal and schedule) will be identified, and solutions evaluated and implemented. Annual agency funding to the various collaborating institutions will be recommended based on discussions with Team Leaders and on the present status and future projections of each task.

Assistant Project Manager: Provide assistance to the Project Manager and act as Project Manager during his/her absence. He/she reports to the Project Manager.

Project Engineer: The Project Engineer will provide project engineering and system engineering for the project. He/she reports to the Project Manager. He/she will have special responsibility for quality control, system engineering, task interfacing, site coordination.

Administrative Assistant: He/she will maintain the project schedule and WBS.

6.2.2 Groups and Sub-Projects

The project has been broken up into four groups and nineteen Sub-projects. The Sub-projects are the working units and it is the responsibility of the Sub-project Leader to ensure that the Sub-project completes its task in a timely and economic fashion. The Sub-project Leader reports to the Project Office on matters of finance, schedule and quality. The Group Coordinator has the responsibility for coordination of activities and technical interfaces between Sub-projects within the Group. The Group Coordinators and Sub-project Leaders are identified in Figure 20.

6.3 Organization Chart

The project will be organized as shown in Figure 20.

6.3.1 Telescope Time Allocation Committee

A telescope Time Allocation Committee will be set up to allot observing time. Each major contributing group will nominate one member to the committee and two members will be selected by the VEC from the general community. All collaboration members can submit observing proposals (some of which may be in collaboration with non-collaboration members). Each observing season the committee will allot time in accordance with the scientific merit of the proposals.

7 Budget and Schedule

This core proposal will be used by the collaborating organizations to individually develop funding proposals to their respective funding agencies.

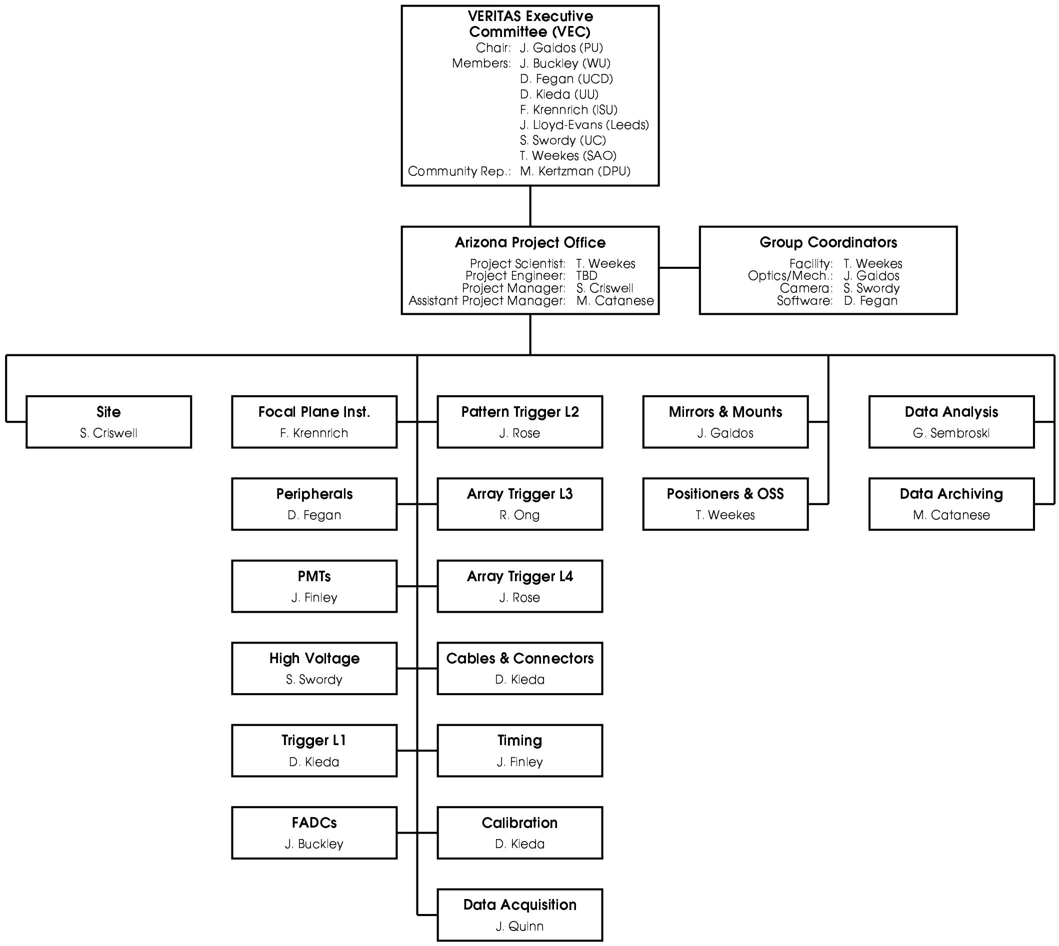

Figure 20: Organizational structure of the VERITAS project.

7.1 Cost Estimate

Facility	$4,593k
Mirrors	$2,443k
OSS, Covers, & Positioners	$3,521k
Peripherals & Slow Control	$146k
PMTs & Bases	$1,223k
High Voltage	$747k
Focalplane Instrumentation	$940k
Telescope Trigger (L1)	$308k
Flash ADC	$3,054k
Telescope Pattern Trigger (L2)	$732k
Central Array Trigger (L3)	$173k
Central Array Pattern Trigger (L4)	$196k
Cables & Connectors	$253k
Timing	$84k
Calibration	$522k
Data Acquisition	$367k
Data Analysis	$35k
Data Archiving	$136k
Project Office	$1,294k
Total	$20,768k

7.1.1 Potential Sources of Funding

These are summarized in Table 2.

Table 2: Potential Sources of VERITAS Funding

Agency	Country	Institutions	Funding by Year ($M) FY00	FY01	FY02	FY03	FY04	Total ($M)
Smithsonian	USA	SAO	0.27	0.06	1.62	4.00	0.42	6.37
DOE	USA	SAO Purdue U. Iowa State U. Washington U.	2.52	1.32	1.45	1.28	0.81	7.38
NSF	USA	U. Utah U. Chicago	0.42	1.22	1.70	1.52	1.09	5.95
PPARC	UK	U. Leeds	0.22	0.17	0.09	0.27	0.17	0.93
Enterprise-Ireland	Ireland	UCD NUI	0.06	0.03	0.03	0.03	0.00	0.15

* The SAO contribution will be partially for the facility ($4.3M) and partially for Major Scientific Instrumentation ($1.9M).

7.2 Site and Facilities

An extensive survey of possible sites for VERITAS in the vicinity of the Whipple Observatory was made in 1998. Two attractive sites were studied by a local architectural firm and application has been made to the Forestry Service for either of these sites. Figure 21 shows the location of the selected sites relative to the observatory. These sites were selected because they are:

- well shielded from current and future Santa Cruz Valley sky brightness,
- topographically flat,
- nearby and can be supported from the FLWO base camp,
- near existing power lines,
- near existing roads,
- adjacent to, but not in, a wilderness area, and
- within line-of-sight to the observatory microwave transmitter.

7.3 Schedule

VERITAS can be completed by September 30, 2004 if funding is available as requested. The schedule will be:

FY00, Phase I (First Reflector initiated): Contracts for the first reflector (optical support structure and positioner), the first camera and the required mirrors will be prepared for letting the following year.

FY01, Phase I (First Reflector: Performance Verification): The first reflector (optical support structure and positioner), the first camera, the first set of electronics and the required mirrors will be manufactured. The prototype unit will be evaluated and design of subsequent units modified as needed.

FY02, Phase II (Add two telescopes): Contracts for the manufacture of the components of reflectors 2 and 3 will be prepared. Reflectors 2 and 3, along with their cameras, electronics and mirrors, will be manufactured and installed.

FY03, Phase III (Add two telescopes): Reflectors 4 and 5 along with their cameras, electronics and mirrors, will be manufactured and installed.

FY04, Phase IV (Add two telescopes): Reflectors 6 and 7 along with their cameras, electronics and mirrors, will be manufactured and installed.

FY05, Phase V (Array verification and operation): The full array will be tested and qualified for routine operation.

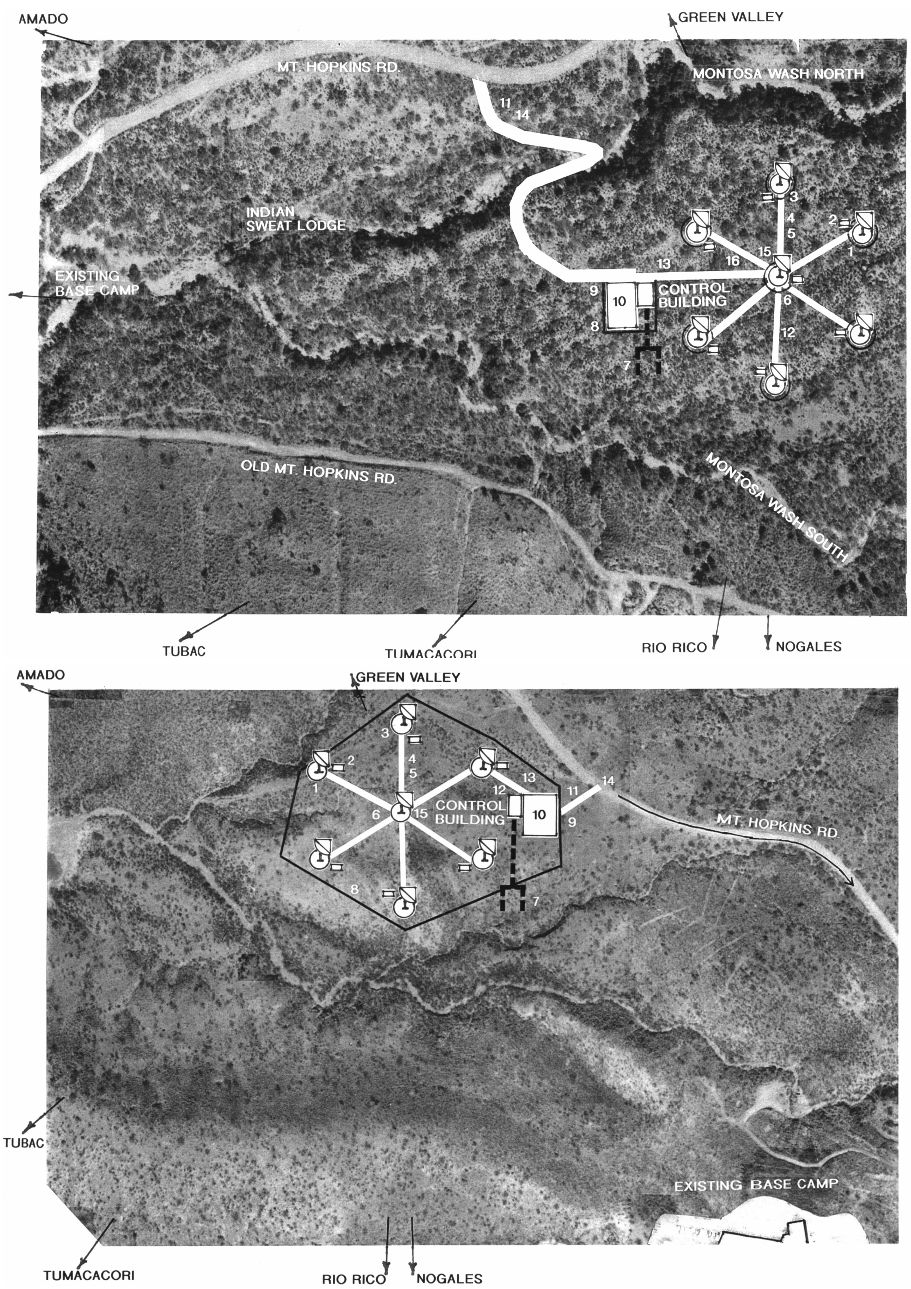

Figure 21: Aerial photographs of the two selected sites for VERITAS in the vicinity of the Whipple Observatory Basecamp with the array superimposed. The top site is in Montosa Canyon and the bottom is north of the Basecamp.

8 VERITAS Outreach

VERITAS will be part of the Smithsonian Institution's Whipple Observatory and thus will share in the public outreach program of the Smithsonian, both locally and nationally. From its inception in 1968 the Whipple Observatory has had a vigorous program of public information with one full-time local staff member devoted to this activity. The well-equipped Visitor Center at the Basecamp Administrative Complex attracts many visitors; bus tours to the observatory are operated three days a week; a public lecture series has been in operation for 28 years and attracts audiences of 300 to 400.

With seven large optical telescopes in an accessible and visually attractive location, we can expect intense public interest in VERITAS. Because of its location close to the Whipple Basecamp and at the end of a double-lane paved road VERITAS will be a good vehicle to expose high energy astronomy and high energy physics to a wider audience. For security reasons we will enclose the VERITAS telescopes by chainlink fences but we will ensure that the telescope closest to the entrance has public viewing access with suitable bilingual displays to explain the nature of the research.

Each of the members of the VERITAS collaboration has an active outreach program in its local community. The University of Chicago group has a close association with the Adler Planetarium and Astronomy Museum. The University of Utah is an active participant in the Aspire Project.

REFERENCES

Aharonian, F.A., & Atoyan, A.M. 1999, A&A, 351, 330

Aiso, S., et al. 1997, Proc. 25th ICRC (Durban), eds. M. S. Potgeier, et al. 5, 373

Amelino-Camelia, G., et al. 1998, Nature, 383, 319

Amenomori, M., et al. 1997, Proc. 25th ICRC (Durban), eds. M. S. Potgeier, et al. 5, 245

Baring, M., et al. 1999, ApJ, 513, 311

Barrau, A., et al. 1998, NIM A, 416, 278

Barrio, J.A., et al. 1998, "The Magic Telescope", design study (MPI-PhE/98-5)

Bergström, L., Ullio, P., & Buckley, J.H. 1998, Astropart. Phys., 9, 137

Biller, S.D., et al. 1998, Phys. Rev. Lett., 80, 2992

Biller, S.D., et al. 1999, Phys. Rev. Lett., 83, 2108

Blandford, R.D., & Ostriker, J.P. 1978, ApJ, 221, L29

Buckley, J.H. 1998, Science, 279, 676

Buckley, J.H., et al. 1996, ApJ, 472, L9

Buckley, J.H., et al. 1998, A&A, 329, 639

Catanese, M. 1999, in BL Lac Phenomenon (Turku, Finland), PASP Conf. Series, 159, 243

Catanese, M., & Weekes, T.C. 1999, PASP, 111, 1193

Catanese, M., et al. 1997, ApJ, 487, L143

Cawley, M.F., et al. 1990, Exp. Astron., 1, 173

Chadwick, P.M., et al. 1998, Astropart. Phys., 9, 131

Chantell, M.C., et al. 1998, NIM A, 408, 468

Davies, J.M., & Cotton, E.S. 1957, J. Solar Energy Sci. and Eng., 1, 16

Drury, L.O'C., Aharonian, F.A., & Völk, H.J. 1994, A&A, 287, 959

Dwek, E., & Slavin, J. 1992, ApJ, 436, 696

Esposito, J.A., et al. 1996, ApJ, 461, 820

Gaidos, J.A., et al. 1996, Nature, 383, 319

Gaisser, T.K., Protheroe, R.J., & Stanev, T. 1998, ApJ, 492, 219

Gawiser, E., & Silk, J. 1998, Science, 280, 1405

Gehrels, N., & Michelson, P. 1999, in TeV Astrophysics of Extragalactic Sources, Astropart. Phys., 11, 277

Georganopoulos, M., & Marscher, A.P. 1998, ApJ, 506, 621

Ghisellini, G. 1999, in TeV Astrophysics of Extragalactic Sources, Astropart. Phys., 11, 11

Ghisellini, G., et al. 1998, MNRAS, 301, 451

Giebels, B., et al. 1998, NIM A, 412, 329

Gould, R. P., & Schréder, G.P. 1967, Phys. Rev., 155, 1408

Hagedorn, R. 1968, Nuovo Cim., LVI A Nr. 4, 1027

Halzen, F., et al. 1991, Nature, 353, 807

Hara, T., et al. 1993, NIM A, 332, 300

Hartman, R.C., et al. 1999, ApJS, 123, 79

Hawking, S.W. 1971, MNRAS, 152, 75

Hillas, A.M. 1996, Space Sci. Rev., 75, 117

Hillas, A.M., et al. 1998, ApJ, 503, 744

Hunter, S.D., et al. 1997, ApJ, 481, 205

Hurley, K. 1994, Nature, 372, 652

Jaffe, T.R., et al. 1997, ApJ, 484, L129

Kamionkowski, M. 1998, Science, 280, 1397

Kifune, T., et al. 1995, ApJ, 438, L91

Konopelko, A. 1999, in TeV Astrophysics of Extragalactic Sources, Astropart. Phys., 11, 263

Konopelko, A., et al. 1999, Astropart. Phys., 10, 275

Koyama, M., et al. 1995, Nature, 378, 255

Krennrich, F., et al. 1998, Astropart. Phys., 8, 213

Krennrich, F., et al. 1999a, ApJ, 511, 149

Krennrich, F., Le Bohec, S., Weekes, T.C. 1999b, ApJ, in press (astro-ph/9909078)

Lamb, R.C., & Macomb, D.J. 1997, ApJ, 488, 872

Macomb, D.J., et al. 1995, ApJ, 449, L99

Malkan, M.A., & Stecker, F.W. 1998, ApJ, 496, 13

Mannheim, K. 1993, A&A, 269, 67

Matsubara, Y. 1997, Towards a Major Atmospheric Čerenkov Detector - V (Kruger Park), ed. O.C. de Jager, 447

McEnery, J.E., et al. 1999, in GeV-TeV Astrophysics: Towards a Major Atmospheric Cherenkov Detector VI (Snowbird), in press (astro-ph/9910549)

Mohanty, G., et al. 1998, Astropart. Phys., 9, 15

Navarro, J.F., Frenk, C.S., & White, S.D.M. 1996, ApJ, 462, 563

Ong, R.A. 1998, Phys. Rep., 305, 93

Page, D.N., & Hawking, S.W. 1976, ApJ, 206, 1

Primack, J.R. 1998, Science, 280, 1398

Primack, J.R., et al. 1999, in TeV Astrophysics of Extragalactic Sources, Astropart. Phys., 11, 93

Protheroe, R.J., et al. 1997, Proc. 25th ICRC (Durban), eds. M. S. Potgeier, et al. 8, 317

Quebert, J., et al. 1995, in Towards a Major Atmospheric Cherenkov Detector IV (Padova), ed. M. Cresti, 248

Quinn, J., et al. 1998, ApJ, 518, 693

Sinnis, G., et al. 1995, Nucl. Phys. B (Proc. Suppl.), 43, 141

Stecker, F.W., & de Jager, O.C. 1998, A&A, 334, L85

Sturner, S.J., & Dermer, C.D. 1995, A&A, 293, L17

Swordy, S.E., et al. 1990, ApJ, 349, 625

Tanimori, T., et al. 1998, ApJ, 497, L25

Thompson, D.J., et al. 1993, ApJS, 86, 629

Vacanti, G., et al. 1991, ApJ, 377, 467

Vassiliev, V.V. 1999, Astropart. Phys., in press (astro-ph/9908088)

Weekes, T.C. 1999, in GeV-TeV Astrophysics: Towards a Major Atmospheric Cherenkov Detector VI (Snowbird), in press (astro-ph/9910394)

Weekes, T.C., & Turver, K.E. 1977, Proc. 12th ESLAB Symp. (Frascati), 279

Weekes, T.C., et al. 1989, ApJ, 342, 370

Witten, E. 1996, Nucl. Phys. B, 471, 135

Yoshikoshi, T., et al. 1997, ApJ, 487, L65